Fraunhofer
ITWM

J. Linn, H. Lang, A. Tuganov

Geometrically exact Cosserat rods with Kelvin-Voigt type viscous damping

Vorwort

Das Tätigkeitsfeld des Fraunhofer-Instituts für Techno- und Wirtschaftsmathematik ITWM umfasst anwendungsnahe Grundlagenforschung, angewandte Forschung sowie Beratung und kundenspezifische Lösungen auf allen Gebieten, die für Techno- und Wirtschaftsmathematik bedeutsam sind.

In der Reihe »Berichte des Fraunhofer ITWM« soll die Arbeit des Instituts kontinuierlich einer interessierten Öffentlichkeit in Industrie, Wirtschaft und Wissenschaft vorgestellt werden. Durch die enge Verzahnung mit dem Fachbereich Mathematik der Universität Kaiserslautern sowie durch zahlreiche Kooperationen mit internationalen Institutionen und Hochschulen in den Bereichen Ausbildung und Forschung ist ein großes Potenzial für Forschungsberichte vorhanden. In die Berichtreihe werden sowohl hervorragende Diplom- und Projektarbeiten und Dissertationen als auch Forschungsberichte der Institutsmitarbeiter und Institutsgäste zu aktuellen Fragen der Techno- und Wirtschaftsmathematik aufgenommen.

Darüber hinaus bietet die Reihe ein Forum für die Berichterstattung über die zahlreichen Kooperationsprojekte des Instituts mit Partnern aus Industrie und Wirtschaft.

Berichterstattung heißt hier Dokumentation des Transfers aktueller Ergebnisse aus mathematischer Forschungs- und Entwicklungsarbeit in industrielle Anwendungen und Softwareprodukte – und umgekehrt, denn Probleme der Praxis generieren neue interessante mathematische Fragestellungen.

Prof. Dr. Dieter Prätzel-Wolters
Institutsleiter

Kaiserslautern, im Juni 2001

Geometrically exact Cosserat rods with Kelvin–Voigt type viscous damping

Joachim Linn[*], **Holger Lang**[#]**, Andrey Tuganov**[*]

[*] Fraunhofer ITWM
Fraunhofer–Platz 1, D–67663 Kaiserslautern, Germany
[joachim.linn, andrey.tuganov]@itwm.fraunhofer.de

[#] Chair of Applied Dynamics
Universität Erlangen–Nürnberg
Konrad–Zuse–Str. 3-5, D–91052 Erlangen, Germany
holger.lang@ltd.uni-erlangen.de

ABSTRACT

We present the derivation of a simple viscous damping model of Kelvin–Voigt type for geometrically exact Cosserat rods from three–dimensional continuum theory. Assuming a homogeneous and isotropic material, we obtain explicit formulas for the damping parameters of the model in terms of the well known stiffness parameters of the rod and the retardation time constants defined as the ratios of bulk and shear viscosities to the respective elastic moduli. We briefly discuss the range of validity of our damping model and illustrate its behaviour with a numerical example.

1 INTRODUCTION

Simulation models for computing the transient response of structural members to dynamic excitations [4] should contain a good approach to account for *dissipative effects* in order to be useful in realistic applications. If the structure considered may be treated within the range of linear dynamics with small vibration amplitudes, there is a well established set of standard approaches, e.g. Rayleigh damping, or a more general modal damping ansatz, to add such effects on the level of discretized versions of linear elastic structural models. In the case of geometrically exact structure models for rods and shells, such linear approaches are not applicable. Here the proper approach to model viscous damping requires the inclusion of a *frame–indifferent viscoelastic constitutive model* into the continuum formulation of the structure model that is capable of dealing with large displacements and finite rotations.

Viscous Kelvin–Voigt damping for Cosserat rods

In our recent work [7], following general considerations of Antman [3] about the functional form of viscoelatic constitutive laws for Cosserat rods, we suggested the possibly simplest model of this kind to introduce *viscous material damping* in our quaternionic reformulation of Simo's dynamic continuum model for Cosserat rods [10] by adding viscous contributions to the material stress resultants $\mathbf{F}$ and stress couples $\mathbf{M}$, which we assumed to be proportional to the *rates* of the material strain measures $\mathbf{U}$ and $\mathbf{V}$ of the rod:

$$\mathbf{F} \;=\; \hat{\mathbb{C}}_F \cdot (\mathbf{V} - \mathbf{V}_0) \;+\; \hat{\mathbb{V}}_F \cdot \partial_t \mathbf{V} \;, \quad \mathbf{M} \;=\; \hat{\mathbb{C}}_M \cdot (\mathbf{U} - \mathbf{U}_0) \;+\; \hat{\mathbb{V}}_M \cdot \partial_t \mathbf{U} \;. \tag{1}$$

The configuration variables of a Cosserat rod [3] are its *centerline* curve $\boldsymbol{\varphi}(s,t)$ and *"moving frame"* $\hat{\mathbf{R}}(s,t) = \mathbf{a}^{(k)}(s,t) \otimes \mathbf{e}_k$ of orthonormal director vectors, both smooth functions of the curve parameter s and the time t, with the pair $\{\mathbf{a}^{(1)}, \mathbf{a}^{(2)}\}$ of directors spanning the local (plane and rigid) cross sections with normals $\mathbf{a}^{(3)}$ along the rod. The material strain measures associated to this configuration are given by *(i)* the components $V_k = \mathbf{a}^{(k)} \cdot \partial_s \boldsymbol{\varphi}$ of the tangent vector in the local frame (i.e.: $\mathbf{V} = \hat{\mathbf{R}}^T \cdot \partial_s \boldsymbol{\varphi} = V_k \mathbf{e}_k$), with V_1, V_2 measuring transverse shear deformation and V_3 measuring (extensional) dilatation, and *(ii)* the *material Darboux vector* $\mathbf{U} = \hat{\mathbf{R}}^T \cdot \mathbf{u} = U_k \mathbf{e}_k$, obtained from its spatial counterpart $\mathbf{u} = U_k \mathbf{a}^{(k)}$ governing the Frénet equations $\partial_s \mathbf{a}^{(k)} = \mathbf{u} \times \mathbf{a}^{(k)}$ of the frame directors, with U_1, U_2 measuring bending curvature w.r.t. the director axes $\{\mathbf{a}^{(1)}, \mathbf{a}^{(2)}\}$, and U_3 measuring torsional twist around the cross section normal. In general, the *reference configuration* of the rod, given by its centerline $\boldsymbol{\varphi}_0(s)$ and frame

$\hat{\mathbf{R}}_0(s) = \mathbf{a}_0^{(k)}(s) \otimes \mathbf{e}_k$, may have non–zero curvature and twist (i.e. $\mathbf{U}_0 \neq \mathbf{0}$). However we may assume zero initial shear ($V_{01} = V_{02} = 0$), such that all cross sections of the reference configuration are orthogonal to the centerline tangent vector, which coincides with the cross section normal (i.e.: $\partial_s \boldsymbol{\varphi}_0 = \mathbf{a}_0^{(3)} \Leftrightarrow V_{03} = 1$) if we choose the arc–length of the reference centerline as curve parameter s.

In the material constitutive equations (1) the elastic properties of the rod are determined by the effective stiffness parameters contained in the symmetric 3×3 matrices $\hat{\mathbb{C}}_F$ and $\hat{\mathbb{C}}_M$. For homogeneous isotropic materials, both matrices are diagonal and given by:

$$\hat{\mathbb{C}}_F = \operatorname{diag}\left(GA\kappa_1, GA\kappa_2, EA\right) \;, \quad \hat{\mathbb{C}}_M = \operatorname{diag}\left(EI_1, EI_2, GI_3\right) \;,$$

with stiffness parameters given by the elastic moduli E and G, geometric parameters of the cross section (area A and geometric moments I_k), and dimensionless shear correction factors κ_j of $\mathcal{O}(1)$ that also depend on the cross section geometry[1]. In [7] we assumed a similar structure for the matrices $\hat{\mathbb{V}}_F$ and $\hat{\mathbb{V}}_M$, which determine the viscous response:

$$\hat{\mathbb{V}}_F = \operatorname{diag}\left(\gamma_{S1}, \gamma_{S2}, \gamma_E\right) \;, \quad \hat{\mathbb{V}}_M = \operatorname{diag}\left(\gamma_{B1}, \gamma_{B2}, \gamma_T\right) \;. \tag{2}$$

The set of six *effective viscosity parameters* γ_{xx} introduced in (2) represents the *integrated cross-sectional viscous damping behaviour* associated to the basic deformation modes (bending, twisting, shearing and extension) of the rod, in the same way as the well known set of stiffness parameters given above determines the corresponding elastic response. Apart of such considerations, Antman [2] suggested a damping model as given by eqns. (1) with positive parameters (2) from a different viewpoint, namely as a simple possibility to introduce dissipative terms (*artificial viscosity*) into the dynamic balance equations of a Cosserat rod, which are a nonlinear coupled hyperbolic system of PDEs, and thereby achieve a regularization effect in view of the possible formation of shock waves that might appear in the undamped hyperbolic equations.

Damping parameter formulas

However, in [2] as well as in [7] the damping parameters γ_{xx} were left undetermined w.r.t. their specific dependence on material and geometric properties. In the case of homogeneous and isotropic material properties, they certainly cannot be independent, but rather should be mutually related in a similar way as the stiffness parameters of the rod in terms of two material parameters (E,G) and the geometrical quantities (A,I_k) associated to the cross section. In fact, we will show that they are given by

$$\frac{\gamma_{S1/2}}{A\kappa_{1/2}} = \frac{\gamma_T}{I_3} = \eta \;, \quad \frac{\gamma_E}{A} = \frac{\gamma_{B1/2}}{I_{1/2}} = \zeta(1-2\nu)^2 + \frac{4}{3}\eta(1+\nu)^2 =: \eta_E \;, \tag{3}$$

where ζ and η are the *bulk and shear viscosities* of a viscoelastic *Kelvin–Voigt solid* [8] with elastic moduli G and $E = 2G(1+\nu)$. While the viscous damping of the deformation modes of pure shear type is solely affected by shear viscosity η, extensional and bending deformations are both associated to normal stresses in the direction orthogonal to the cross section, which are damped by a specific combination of both bulk and shear viscosity that depends on the compressibilty of the material and may be interpreted as *extensional viscosity* parameter η_E. Introducing the *retardation time* constants $\tau_S = \eta/G$ and $\tau_B = \zeta/K$, which relate the viscosities η and ζ to the shear and bulk moduli G and $3K = E/(1-2\nu)$, as well as the time constant $\tau_E = \eta_E/E$, which analogously relates the extensional viscosity to Young's modulus, the formulas (3) may be equivalently rewritten as

$$\frac{\gamma_{S1/2}}{GA\kappa_{1/2}} = \frac{\gamma_T}{GI_3} = \tau_S \;, \quad \frac{\gamma_E}{EA} = \frac{\gamma_{B1/2}}{EI_{1/2}} = \frac{1}{3}\left[(1-2\nu)\tau_B + 2(1+\nu)\tau_S\right] = \tau_E \tag{4}$$

in terms of the stiffness parameters of the rod and the retardation time constants. For a given rod consisting of homogeneous and isotropic material, one may first determine the elastic moduli G and E by standard tests (i.e.: twisting, uniaxial extension of 3–point–bending of the rod with small deformation amplitudes), and after that measure the time constants by observing relaxation oscillations or cylic data at sufficiently low frequencies (see [8]). Interesting special cases of (4) are the simplified expressions $\eta_E = \zeta + \frac{4}{3}\eta$, $\tau_E = \frac{1}{3}(\tau_B + 2\tau_S)$ for completely compressible materials[2] (i.e. $\nu = 0$), and $\eta_E = 3\eta$, $\tau_E = \tau_S$ for incompressible materials[3] ($\nu = \frac{1}{2}$). For $\tau_B = \tau_S$ we obtain $\tau_E = \tau_{B/S}$ independent of the value of ν.

---

[1] If out–of–plane cross section warping is not negligible, GI_3 should be replaced by an improved torsional stiffness parameter.

[2] The formulas given in the extended abstract are valid only for this case.

[3] Note that the latter relation between shear and extensional viscosity is well known for incompressible Newtonian fluids.

Overview of the remaining sections of the paper

In the following section, we will present a derivation of the formulas (3) from 3D continuum theory in analogy to the derivation of the elastic energy (or *stored energy function*)

$$W_{el} \;=\; \int_0^L ds \, \frac{1}{2} \left[(\mathbf{V} - \mathbf{V}_0)^T \cdot \hat{\mathbb{C}}_F \cdot (\mathbf{V} - \mathbf{V}_0) \;+\; (\mathbf{U} - \mathbf{U}_0)^T \cdot \hat{\mathbb{C}}_M \cdot (\mathbf{U} - \mathbf{U}_0) \right] \tag{5}$$

of a Cosserat rod. The analogous procedure for the viscous part results in the derivation of the *dissipation function* of a Cosserat rod as introduced[4] in [7]

$$W_{visc} \;=\; \int_0^L ds \, \frac{1}{2} \left[\partial_t \mathbf{V}^T \cdot \hat{\mathbb{V}}_F \cdot \partial_t \mathbf{V} \;+\; \partial_t \mathbf{U}^T \cdot \hat{\mathbb{V}}_M \cdot \partial_t \mathbf{U} \right] \tag{6}$$

from the 3D (volumetric) dissipation function of a Kelvin–Voigt solid [6, 8]. At the end of the section we briefly discuss the validity of the Kelvin–Voigt model. We also comment on the relation of our continuum model to the Kelvin–Voigt type model recently proposed in [1] for usage within an alternative discretized approach to geometrically nonlinear rods using the *absolute nodal coordinate formulation* (ANCF).

In the third section, we will illustrate the behaviour of our Kelvin–Voigt type viscous damping model (1) by simple numerical experiments. We conclude our paper with a short summary.

2 DERIVATION OF THE KELVIN–VOIGT MODEL FOR COSSERAT RODS

In order to set the notational and conceptional framework for the derivation of the viscous part of our damping model, we first give a brief account of the derivation of its elastic part, i.e.: the stored energy function (5) of a Cosserat rod. Within this derivation we will encounter a variety of smallness assumptions w.r.t. the curvatures describing the reference geometry of the rod as well as the local strains occuring in its deformed configurations. In our subsequent derivation of the viscous dissipation function (6) we will use the same assumptions and thereby remain consistent with the derivation of the elastic part.

2.1 Basic Cosserat rod kinematics

Introducing cartesian coordinates (ξ_1, ξ_2) w.r.t. the director basis $\{\mathbf{a}_0^{(1)}(s), \mathbf{a}_0^{(2)}(s)\}$ chosen in the cross section located at the centerline point $\boldsymbol{\varphi}_0(s)$, the spatial positions of material points in the reference configuration of the rod are given by[5]

$$\mathbf{X}(\xi_1, \xi_2, s) \;=\; \boldsymbol{\varphi}_0(s) \;+\; \xi_\alpha \, \mathbf{a}_0^{(\alpha)}(s) \,. \tag{7}$$

The positions of the same material points in the current (deformed) configuration are then given by

$$\mathbf{x}(\xi_1, \xi_2, s, t) \;=\; \boldsymbol{\varphi}(s, t) \;+\; \xi_\alpha \, \mathbf{a}^{(\alpha)}(s, t) \;+\; \mathbf{w}(\xi_1, \xi_2, s, t) \tag{8}$$

in terms of the deformed centerline curve $\boldsymbol{\varphi}(s, t)$, the rotated orthonormal cross section basis vectors $\{\mathbf{a}^{(1)}(s, t), \mathbf{a}^{(2)}(s, t)\}$, the same pair of cartesian cross section coordinates (ξ_1, ξ_2), and an additional displacement vector field $\mathbf{w}(\xi_1, \xi_2, s, t)$, which by definition describes the (in–plane and out–of–plane) *warping* deformations of the cross sections along the deformed rod.

The kinematic assumption that the cross sections of a rod remain plane and rigid in a configuration is equivalent to the assumption that the displacement field $\mathbf{w}$ vanishes identically. Although we will initially adhere to this very common assumption for rod models, we will later admit some specific form of in–plane deformation of cross sections — namely: a *uniform lateral contraction* — to correct a deficiency caused by the overly rigid kinematical ansatz (8) with $\mathbf{w} \equiv \mathbf{0}$.

---

[4]Note that in [7] (compare eqns. (9) and (10) in sec. 2.2) we absorbed the prefactor $1/2$ into the definition (2) of the damping parameters, which leads to an additional factor of 2 multiplying $\hat{\mathbb{V}}_F$ and $\hat{\mathbb{V}}_M$ in the constitutive equations (1) of the rod model.

[5]Within this paper we make use of Einstein's summation convention — as the reader may have observed already — w.r.t. all indices occuring twice within *product* terms, with greek indices $\alpha, \beta, \ldots$ running from 1 to 2 and latin ones $i, j, k, \ldots$ from 1 to 3.

For simplicity we assume the rod to be *prismatic*, such that all cross sections along the rod are identical, and the domain of the cartesian coordinates (ξ_1, ξ_2) coincides with one fixed domain $\mathcal{A} \subset \mathbb{R}^2$. As usual we choose the geometrical center of the domain $\mathcal{A}$ to coincide with the origin of $\mathbb{R}^2$ such that $\langle \xi_\alpha \rangle_{\mathcal{A}} = 0$ holds, where we introduced the shorthand notation $\langle f \rangle_{\mathcal{A}} := \int_{\mathcal{A}} f(\xi_1, \xi_2) \, d\xi_1 d\xi_2$ for the *cross section integral* of functions. In addition we choose the orientation of the orthonormal director pairs $\{\mathbf{a}_0^{(1)}(s), \mathbf{a}_0^{(2)}(s)\}$ as well as $\{\mathbf{a}^{(1)}(s,t), \mathbf{a}^{(2)}(s,t)\}$ to coincide with the principle geometrical axes of $\mathcal{A}$, such that $\langle \xi_1 \xi_2 \rangle_{\mathcal{A}} = 0$ holds. The quantities that characterize the geometric properties of the cross section in the Cosserat rod model are the *cross section area* $A = \langle 1 \rangle_{\mathcal{A}}$, the two *area moments* $I_1 = \langle \xi_2^2 \rangle_{\mathcal{A}}$, $I_2 = \langle \xi_1^2 \rangle_{\mathcal{A}}$ and the *polar area moment* $I_3 = \langle \xi_1^2 + \xi_2^2 \rangle_{\mathcal{A}} = I_1 + I_2$.

2.2 Three–dimensional strain measures of a Cosserat rod

In the next step we compute the *deformation gradient* $\hat{\mathbf{F}} = \mathbf{g}_k \otimes \mathbf{G}^k$, the *right Cauchy–Green tensor* $\hat{\mathbf{C}} = \hat{\mathbf{F}}^T \cdot \hat{\mathbf{F}}$ and the *Green–Lagrange strain tensor* $\hat{\mathbf{E}} = \frac{1}{2}(\hat{\mathbf{C}} - \hat{\mathbf{I}})$ from the basis vectors $\mathbf{G}_k = \partial_k \mathbf{X}$ and $\mathbf{g}_k = \partial_k \mathbf{x}$ associated to the curvilinear coordinates of the rod configurations given by (7) and (8), with $\partial_k = \frac{\partial}{\partial \xi_k}$ for $k = 1, 2$ and $\partial_3 = \partial_s$ for $\xi_3 = s$. The dual basis vectors $\mathbf{G}^j$ and $\mathbf{g}^j$ are defined by the relations $\mathbf{G}_i \cdot \mathbf{G}^j = \delta_{ij}$ and $\mathbf{g}_i \cdot \mathbf{g}^j = \delta_{ij}$ respectively. Proceeding in this way we obtain the basis vectors of the reference configuration (7) as $\mathbf{G}_\alpha = \mathbf{a}_0^{(\alpha)}(s)$ and $\mathbf{G}_3 = \mathbf{a}_0^{(3)}(s) + \xi_\alpha U_{0\alpha}(s) \mathbf{a}_0^{(\alpha)}(s)$. Their duals may be computed from the general formula $\mathbf{G}^i = \mathbf{G}^j \times \mathbf{G}^k / J_0$ with $J_0 := (\mathbf{G}_1 \times \mathbf{G}_2) \cdot \mathbf{G}_3$, where (ijk) is a cyclic permutation of the indices (123), with the result:

$$\mathbf{G}^1 = \mathbf{a}_0^{(1)}(s) + \xi_2 \frac{U_{03}(s)}{J_0(s)} \mathbf{a}_0^{(3)}(s) \,, \ \ \mathbf{G}^2 = \mathbf{a}_0^{(2)}(s) - \xi_1 \frac{U_{03}(s)}{J_0(s)} \mathbf{a}_0^{(3)}(s) \,, \ \ \mathbf{G}^3 = \frac{1}{J_0(s)} \mathbf{a}_0^{(3)}(s) \,.$$

The inital curvatures $U_{0\alpha}(s)$ contained in the determinant $J_0(s) = 1 + \xi_2 U_{01}(s) - \xi_1 U_{02}(s)$ and the initial twist $U_{03}(s)$ of the reference configuration (7) influence the deviation of the dual vectors $\mathbf{G}^k$ from the frame directors $\mathbf{a}_0^{(k)}(s)$ within the cross section. Both vectors coincide if the reference configuration of the rod is straight and untwisted (i.e.: $\mathbf{U}_0 = \mathbf{0}$). We have approximate coincidence $\mathbf{G}^k \approx \mathbf{a}_0^{(k)}(s)$ if curvature and twist of the reference configuration are sufficiently weak, in the sense that for the curvature radii given by $R_k = 1/|U_{0k}|$ the estimates $|\xi_\alpha|/R_3 \ll 1$ and $|\xi_\alpha|/R_\beta \ll 1 \Rightarrow J_0 \approx 1$ hold throughout each cross section along the rod, such that all initial curvature radii R_α are large compared to the cross section diameter. The geometric approximation $J_0(s) \approx 1$ will occur repeatedly and therefore play an important role in the derivation of the elastic energy and dissipation function of a Cosserat rod. To compute the deformation gradient we also need the basis vectors $\mathbf{g}_\alpha = \mathbf{a}^{(\alpha)}(s,t)$ and $\mathbf{g}_3 = \mathbf{a}^{(3)}(s,t) + \xi_\alpha U_\alpha(s,t) \mathbf{a}^{(\alpha)}(s,t)$ of the deformed configuration (8) with vanishing warping vector field ($\mathbf{w} = 0$). For the dual vectors $\mathbf{g}^k$ one obtaines analogous expressions as those for the dual vectors $\mathbf{G}^k$ given above, which we omit here.

For the special kinematical relations of a Cosserat rod, the deformation gradient $\hat{\mathbf{F}} = \mathbf{g}_k \otimes \mathbf{G}^k$ may be expressed in terms of a *pseudo–polar decomposition* [5] by a factorization of the *relative rotation* $\hat{\mathbf{R}}_{rel}(s,t) := \hat{\mathbf{R}}(s,t) \cdot \hat{\mathbf{R}}_0^T(s) = \mathbf{a}^{(k)}(s,t) \otimes \mathbf{a}_0^{(k)}(s)$ connecting the moving frames of the reference and deformed configurations of the rod. The resulting formula

$$\hat{\mathbf{F}}(\xi_1, \xi_2, s, t) = \hat{\mathbf{R}}_{rel}(s,t) \left[\hat{\mathbf{I}} + \frac{1}{J_0(s)} \mathbf{H}(\xi_1, \xi_2, s, t) \otimes \mathbf{a}_0^{(3)}(s) \right] \tag{9}$$

depends on the *absolute values* of the curvatures of the reference configuration (7) through $J_0(s)$, and on the *change of the strain measures* of the Cosserat rod given by the difference vectors $\mathbf{U} - \mathbf{U}_0$ and $\mathbf{V} - \mathbf{V}_0 = (V_1, V_2, V_3 - 1)^T$ in terms of the *material strain vector* $\mathbf{H} = H_k \mathbf{a}_0^{(k)}$ with components

$$H_1 = V_1(s,t) - \xi_2 \left[U_3(s,t) - U_{03}(s) \right] \,, \ \ H_2 = V_2(s,t) + \xi_1 \left[U_3(s,t) - U_{03}(s) \right]$$
$$H_3 = \left[V_3(s,t) - 1 \right] + \xi_2 \left[U_1(s,t) - U_{01}(s) \right] - \xi_1 \left[U_2(s,t) - U_{02}(s) \right] \,. \tag{10}$$

Our derivation generalizes the treatment given in [5] for the simpler case of a straight and untwisted reference configuration of the rod (i.e. $\mathbf{U}_0 = \mathbf{0}$). Computing the right Cauchy–Green tensor field $\hat{\mathbf{C}} = \hat{\mathbf{F}}^T \cdot \hat{\mathbf{F}}$ with the deformation gradient given by (9) results in the following exact expression[6] for the Green–Lagrange

---

[6]To simplify the notation, we omitted all function arguments here.

strain tensor:

$$\hat{\mathbf{E}} \;=\; \frac{1}{2J_0}\left[\mathbf{H}\otimes\mathbf{a}_0^{(3)}+\mathbf{a}_0^{(3)}\otimes\mathbf{H}\right]\;+\;\frac{\mathbf{H}^2}{2J_0^2}\,\mathbf{a}_0^{(3)}\otimes\mathbf{a}_0^{(3)}\;. \tag{11}$$

The approximate expression

$$\hat{\mathbf{E}} \;\approx\; \frac{1}{2}\left[\mathbf{H}\otimes\mathbf{a}_0^{(3)}+\mathbf{a}_0^{(3)}\otimes\mathbf{H}\right] \tag{12}$$

may be obtained from (11) by the assumption $\|\mathbf{H}\|\ll 1$ of a small material strain vector and the assumption $J_0\approx 1$. Later we will make use of this approximate strain tensor, which is *linear* in the vector field $\mathbf{H}$ and therefore also in the change of the strain measures of the rod, to obtain the stored energy function (5), which becomes a quadratic form in the change of the strain measures. Likewise we will use (12) to obtain an approximation of the strain rate $\partial_t\mathbf{E}$ in terms of the rate $\partial_t\mathbf{H}$ of the strain vector.

For deformed configurations of a slender rod one observes large displacements and rotations, but local strains remain small. To estimate the size of the strain tensor it is useful to compute its components $E_{ij}=\mathbf{a}_0^{(i)}\cdot(\hat{\mathbf{E}}\cdot\mathbf{a}_0^{(j)})$ w.r.t. the tensor basis $\mathbf{a}_0^{(i)}\otimes\mathbf{a}_0^{(j)}$ obtained from the directors of the reference frame $\hat{\mathbf{R}}_0(s)$. From (11) and (12) we obtain the following exact and approximate expressions:

$$E_{\alpha\beta}=E_{\beta\alpha}\equiv 0\;\;,\quad E_{\alpha 3}=E_{3\alpha}=\frac{H_\alpha}{2J_0}\approx\frac{H_\alpha}{2}\;\;,\quad E_{33}=\frac{H_3}{J_0}+\frac{\mathbf{H}^2}{2J_0^2}\approx H_3\;\;. \tag{13}$$

Introducing the the quantity $|\xi|_{max}=\max_{(\xi_1,\xi_2)\in\mathcal{A}}(|\xi_1|,|\xi_2|)$ to estimate the maximal linear extension of the cross section $\mathcal{A}$, one may estimate the deviation of the determinant $J_0(s)$ from unity by $|J_0(s)-1|\leq|\xi|_{max}(1/R_1+1/R_2)$ as a coarse check of the validity of the approximation $J_0\approx 1$. Otherwise the smallness of the components of $\hat{\mathbf{E}}$ is implied by the smallness of the components H_k of the strain vector. According to (10) these components in turn become small if the change of the strain measures of the Cosserat rod is small, i.e. if the estimates $|V_\alpha|\ll 1$, $|V_3-1|\ll 1$, $|U_k-U_{0k}|\ll 1/|\xi|_{max}$ hold. For slender rods with moderately curved undeformed geometry these estimates are obviously easily satisfiable, except for extreme deformations of the rod that produce large curvatures or twists of the order of the inverse cross section diameter. In this case, the assumption of small strains obviously would be invalid.

2.3   Elastic constitutive behaviour of rods at small strains

If we assume the rod material to behave hyperelastically with a stored energy density function $\Psi_{el}(\hat{\mathbf{E}})$, a simple Taylor expansion argument[7] shows that the behaviour of the energy density within the range of small strains may be well approximated by the quadratic function $\Psi_{el}(\hat{\mathbf{E}})\approx\frac{1}{2}\hat{\mathbf{E}}:\widehat{\mathbb{H}}:\hat{\mathbf{E}}$, where $\widehat{\mathbb{H}}=\partial_{\hat{\mathbf{E}}}^2\Psi_{el}(\hat{\mathbf{0}})$ is the fourth order *Hookean material tensor* known from linear elasticity. This quadratic approximation yields a well defined frame–indifferent elastic energy density that is suitable for structure deformations at small local strains, but arbitrary large displacements and rotations, and therefore serves as a proper basis for the derivation of the stored energy function of a Cosserat rod.

The corresponding approximation of the stress–strain relation yields the 2nd *Piola–Kirchhoff stress* tensor $\hat{\mathbf{S}}=\partial_{\hat{\mathbf{E}}}\Psi_{el}(\hat{\mathbf{E}})\approx\widehat{\mathbb{H}}:\hat{\mathbf{E}}$ for small strains. The 1st *Piola–Kirchhoff stress* tensor $\hat{\mathbf{P}}$, which is used to define the stress resultants and stress couples of the Cosserat rod model [10], is obtained by the transformation $\hat{\mathbf{P}}=\hat{\mathbf{F}}\cdot\hat{\mathbf{S}}$ using the deformation gradient, and the Cauchy stress tensor by yet another transformation $\hat{\sigma}=J^{-1}\hat{\mathbf{P}}\cdot\hat{\mathbf{F}}^T$, which contains also $J=\det(\hat{\mathbf{F}})$. If we approximate the strain tensor $\hat{\mathbf{E}}$ by (12) and consistently discard all terms that are of second order in $\|\mathbf{H}\|$ in accordance with our assumption of small strains, we have to use the approximation $\hat{\mathbf{F}}\approx\hat{\mathbf{R}}_{rel}(s)$ (which implies $J\approx 1$) for the deformation gradient in all stress tensor transformations. This means that all pull back or push forward transformations are carried out approximately as a simple (relative) rotation connecting corresponding frames $\hat{\mathbf{R}}_0(s)$ and $\hat{\mathbf{R}}(s,t)$ of the undeformed and deformed configurations of a Cosserat rod. Alltogether we obtain the approximate expressions $\hat{\mathbf{S}}\approx\widehat{\mathbb{H}}:\hat{\mathbf{E}}\;\rightarrow\;\hat{\mathbf{P}}\approx\hat{\mathbf{R}}_{rel}\cdot\hat{\mathbf{S}}\,,\;\hat{\sigma}\approx\hat{\mathbf{R}}_{rel}\cdot\hat{\mathbf{S}}\cdot\hat{\mathbf{R}}_{rel}^T$ for the various stress tensors, which are valid for the specific type of small strain assumptions for Cosserat rods as previously discussed.

In the case of a homogeneous and isotropic material the Hookean tensor acquires the special form of an isotropic fourth order tensor $\widehat{\mathbb{H}}_{SVK}=\lambda\,\hat{\mathbf{I}}\otimes\hat{\mathbf{I}}+2\mu\,\widehat{\mathbb{I}}$ depending on two constant elastic moduli (the *Lamé*

---

[7]Additional assumptions are the vanishing of the elastic energy density at zero strain ($\Psi_{el}(\hat{\mathbf{0}})=0$), as well as the absence of initial stresses in the undeformed configuration (i.e.: $\hat{\mathbf{S}}_0=\partial_{\hat{\mathbf{E}}}\Psi_{el}(\hat{\mathbf{0}})=\hat{\mathbf{0}}$).

parameters λ and μ). Here $\hat{\mathbf{I}}$ and $\widehat{\mathbb{I}}$ are the second and fourth order identity tensors, which act on arbitrary (symmetric) second order tensors $\hat{\mathbf{Q}}$ by double contraction as $\widehat{\mathbb{I}} : \hat{\mathbf{Q}} = \hat{\mathbf{Q}}$ and $\hat{\mathbf{I}} : \hat{\mathbf{Q}} = \text{Tr}(\hat{\mathbf{Q}})$, such that one obtains $\hat{\mathbf{Q}} : (\hat{\mathbf{I}} \otimes \hat{\mathbf{I}}) : \hat{\mathbf{Q}} = \text{Tr}(\hat{\mathbf{Q}})^2$ and $\hat{\mathbf{Q}} : \widehat{\mathbb{I}} : \hat{\mathbf{Q}} = \hat{\mathbf{Q}} : \hat{\mathbf{Q}} = \text{Tr}(\hat{\mathbf{Q}}^2) = \|\hat{\mathbf{Q}}\|_F^2$, where $\|\dots\|_F$ is the Frobenius norm. The corresponding quadratic energy function is the *Saint–Venant Kirchhoff* potential

$$\Psi_{SVK}(\hat{\mathbf{E}}) \;=\; \frac{1}{2}\,\hat{\mathbf{E}} : \widehat{\mathbb{H}}_{SVK} : \hat{\mathbf{E}} \;=\; \frac{\lambda}{2}\,\text{Tr}(\hat{\mathbf{E}})^2 \;+\; \mu\,\|\hat{\mathbf{E}}\|_F^2 \;=\; \frac{K}{2}\,\text{Tr}(\hat{\mathbf{E}})^2 \;+\; \mu\,\|\widehat{\mathbb{P}} : \hat{\mathbf{E}}\|_F^2 \;, \qquad (14)$$

where $\widehat{\mathbb{P}} = \widehat{\mathbb{I}} - \frac{1}{3}\hat{\mathbf{I}} \otimes \hat{\mathbf{I}}$ is the orthogonal projection operator on the subspace of traceless second order tensors, such that $\widehat{\mathbb{P}} : \hat{\mathbf{E}} = \hat{\mathbf{E}} - \frac{1}{3}\text{Tr}(\hat{\mathbf{E}})\hat{\mathbf{I}}$ is the traceless (deviatoric) part of the strain tensor, and $K = \lambda + \frac{2}{3}\mu$ is the *bulk modulus*. The well known stress–strain relation obtained from (14) is given by

$$\hat{\mathbf{S}}_{SVK} \;=\; \partial_{\hat{\mathbf{E}}}\,\Psi_{SVK}(\hat{\mathbf{E}}) \;=\; \lambda\,\text{Tr}(\hat{\mathbf{E}})\,\hat{\mathbf{I}} + 2\mu\,\hat{\mathbf{E}} \;=\; K\,\text{Tr}(\hat{\mathbf{E}})\,\hat{\mathbf{I}} + 2\mu\,\widehat{\mathbb{P}} : \hat{\mathbf{E}} \;. \qquad (15)$$

2.4 Modified strain tensor including uniform lateral contraction effects

Inserting the approximate expressions[8] (12) and (13) of the strain tensor and its components into (15) yields the small strain approximation $\hat{\mathbf{S}}_{SVK} \approx \lambda H_3 \hat{\mathbf{I}} + \mu[\mathbf{H} \otimes \mathbf{a}_0^{(3)} + \mathbf{a}_0^{(3)} \otimes \mathbf{H}]$ of the stress tensor $\hat{\mathbf{S}}_{SVK}$ for Cosserat rods. The computation of the stress components w.r.t. the basis of $\hat{\mathbf{R}}_0(s)$ directors yields normal stress components $S_{\alpha\alpha} \approx \lambda H_3$ and $S_{33} \approx (\lambda + 2\mu)H_3$, and the shear stress components are given by $S_{12} = S_{21} = 0$ and $S_{\alpha 3} = S_{3\alpha} \approx \mu H_\alpha$ respectively.

As the elastic moduli $\lambda = 2\mu\nu/(1-2\nu)$ and $\lambda + 2\mu = 2\mu(1-\nu)/(1-2\nu)$ appearing in the expressions for the normal stress components, expressed in terms of the shear modulus $\mu = G$ and Poisson's ratio given by $2\nu = \lambda/(\lambda + \mu)$, diverge in the incompressible limit $\nu \to \frac{1}{2}$ (just as the bulk modulus $K = \frac{2}{3}\frac{1+\nu}{1-2\nu}G$ does), the normal stresses would become infinitely large whenever the normal strain $E_{33} \approx H_3$ becomes nonzero. This unphysical behaviour clearly is a direct consequence of the kinematical assumption of plain and *rigid* cross section, which e.g. prevents any lateral contraction of the cross section in the case of a longitudinal extension. Therefore the assumption of a perfectly rigid cross section, as well as the expressions (11) and (12) derived under this assumption, are compatible only with perfectly compressible materials ($\nu = 0$).

The standard procedure to fix this deficiency [11] is based on the plausible requirement that *all* in–plane stress components $S_{\alpha\beta}$ (including the normal stresses $S_{\alpha\alpha}$), which for rods in practice are very small compared to the out of plain normal and shear stresses $S_{\alpha 3}$ and S_{33}, should *vanish* completely. This may be achieved by imposing a *uniform lateral contraction* with in–plane normal strain components $E_{\alpha\alpha} = -\nu E_{33}$ upon the cross section. Allthough this procedure seems to be rather ad hoc, it may be justified by an asymptotic analysis of the local strain field for rods, e.g. in the way as presented by A.E.H. Love in the paragraph §256 on the *"Nature of the strain in a bent and twisted rod"* in Ch. XVIII of his book [9]. Following Love's analysis, we obtain the in–plane normal strains to leading order as $E_{\alpha\alpha} = \partial_\alpha w_\alpha = -\nu E_{33}$ with the additional requirement that $E_{12} = E_{21} = \partial_1 w_2 + \partial_2 w_1 = 0$, which determines the in–plane components w_α of the the warping field $\mathbf{w}$ corresponding to the lateral contraction in terms of E_{33}.

To obtain the modified value of $E_{\alpha\alpha} = -\nu E_{33}$ one has to add an additional term $-\nu E_{33}\,\mathbf{a}_0^{(\alpha)} \otimes \mathbf{a}_0^{(\alpha)}$ to the exact expression (11) of the strain tensor. Using the identity $\hat{\mathbf{I}} = \mathbf{a}_0^{(k)} \otimes \mathbf{a}_0^{(k)}$, we obtain the following modified expression for the strain tensor:

$$\hat{\mathbf{E}}' \;=\; \hat{\mathbf{E}} \;-\; \nu\,E_{33}\left[\hat{\mathbf{I}} - \mathbf{a}_0^{(3)} \otimes \mathbf{a}_0^{(3)}\right] \;. \qquad (16)$$

The small strain approximation is obtained by using $E_{33} \approx H_3$ according to (12). Inserting this modified strain tensor (16) into the stress–strain equation of the Saint–Venant–Kirchhoff material with $\text{Tr}(\hat{\mathbf{E}}') = (1 - 2\nu)E_{33} \approx (1 - 2\nu)H_3$, and using the relation $\lambda(1-2\nu) = \frac{\nu}{1+\nu}E$ relating the Lamé parameter λ to Young's modulus E, we obtain the following modified expression for the stress of a Cosserat rod:

$$\hat{\mathbf{S}}'_{SVK} \;\approx\; \frac{E\nu}{1+\nu}\,H_3\,\mathbf{a}_0^{(3)} \otimes \mathbf{a}_0^{(3)} \;+\; G\left[\mathbf{H} \otimes \mathbf{a}_0^{(3)} + \mathbf{a}_0^{(3)} \otimes \mathbf{H}\right] \;. \qquad (17)$$

---

[8]All of the following considerations are likewise valid if the *exact* expression (11) for the strain tensor and its components (13) were used. However, the seemingly more complete formulas obtained in this way would have only formal meaning and seemingly improved accuracy, as we made use of a constitutive model valid for *small* strains only. Therefore we use the *approximate* expressions not only for simplicity, but also to remain consistent with the small strain assumption.

By construction, we now obtain vanishing in–plane stress components $S'_{12} = S'_{21} = S'_{\alpha\alpha} \equiv 0$, while the transverse shear stresses remain unaffected by the modification (i.e.: $S'_{\alpha3} = S'_{3\alpha} \approx G H_\alpha$ with $G = \mu$). As $2G = E/(1 + \nu)$, we obtain the modified expression $S'_{33} \approx E H_3$ for the normal stress component orthogonal to the cross section, which corresponds to the familiar expression from elementary linear beam theory, with the correct modulus E replacing the deficient term $\lambda + 2\mu$.

2.5 Stored energy function of a Cosserat rod

We briefly demonstrate that the modified expressions (16) and (17) immediately lead to the known stored energy function (5) mentioned in the introduction. The stored energy function is obtained by integrating the density (14) over the cross section and along the centerline, i.e.: $W_{el} = \int_0^L ds \left\langle \Psi_{SVK}(\hat{\mathbf{E}}') \right\rangle_\mathcal{A}$, using $\hat{\mathbf{E}}'$ from (16). As

$$\Psi_{SVK}(\hat{\mathbf{E}}') = \frac{1}{2} \hat{\mathbf{S}}'_{SVK} : \hat{\mathbf{E}}' \approx \frac{1}{2} \left[E H_3^2 + G(H_1^2 + H_2^2) \right] ,$$

the cross section integral of the energy density can be computed in terms of the integrals

$$\left\langle H_1^2 + H_2^2 \right\rangle_\mathcal{A} = A(V_1^2 + V_2^2) + I_3(U_3 - U_{03}) , \quad \left\langle H_3^2 \right\rangle_\mathcal{A} = A(V_3 - 1)^2 + I_\alpha(U_\alpha - U_{0\alpha}) .$$

This yields the desired result

$$2\left\langle \Psi_{SVK}(\hat{\mathbf{E}}') \right\rangle_\mathcal{A} \approx EA(V_3 - 1)^2 + GA(V_1^2 + V_2^2) + EI_\alpha(U_\alpha - U_{0\alpha}) + GI_3(U_3 - U_{03}) .$$

Introducing the shear correction factors ($GA \to GA\kappa_\alpha$) finally yields the stored energy function (5).

2.6 Kelvin–Voigt type dissipation function of a Cosserat rod

Now we have collected all material and approximate results that enable us to derive the dissipation function (6) of a Cosserat rod from a three-dimensional Kelvin–Voigt model in analogy to the derivation of the stored energy function (5) in a consistent way.

In [6] (see Ch. V §33) the *dissipation function* $\int_V dV \frac{1}{2}\eta_{ijkl}\dot{\varepsilon}_{ij}\dot{\varepsilon}_{kl}$ was suggested to model dissipative effects within a solid body near thermodynamic equilibrium, with constant fourth order tensor components η_{ijkl} that are the viscous analogon of the Hookean elasticity tensor. Transfering this ansatz to the formalism used in our paper, the dissipation function of [6] becomes that of a *Kelvin–Voigt solid* [8]

$$W_{KV} = \int_0^L ds \left\langle \Psi_{KV}(\partial_t \hat{\mathbf{E}}) \right\rangle_\mathcal{A} , \quad \Psi_{KV}(\partial_t \hat{\mathbf{E}}) = \frac{1}{2} \partial_t \hat{\mathbf{E}} : \widehat{\mathbb{V}} : \partial_t \hat{\mathbf{E}} , \tag{18}$$

which is a quadratic form in the material strain rate $\partial_t \hat{\mathbf{E}}$ defined as the time derivative of the Green–Lagrange strain tensor. The constant fourth order *viscosity tensor* $\widehat{\mathbb{V}}$ may be assumed to have the same symmetries as the Hookean tensor $\widehat{\mathbb{H}}$, with its components depending on *viscosity parameters* in the same way as the components of $\widehat{\mathbb{H}}$ depend on elastic moduli. The stress–strain relation of the Kelvin–Voigt model is given by $\hat{\mathbf{S}} = \widehat{\mathbb{H}} : \hat{\mathbf{E}} + \widehat{\mathbb{V}} : \partial_t \hat{\mathbf{E}}$, with the viscous stress given by the term $\widehat{\mathbb{V}} : \partial_t \hat{\mathbf{E}} = \partial_{\partial_t \hat{\mathbf{E}}} \Psi_{KV}(\partial_t \hat{\mathbf{E}})$.

The dissipation function for a Cosserat rod results by inserting the rate $\partial_t \hat{\mathbf{E}}'$ of the modified strain tensor (16) into the dissipation density function Ψ_{KV} of the Kelvin–Voigt model. We will compute this dissipation function explicitly in closed form for the special case of a *homogeneous and isotropic* material. In this case, the viscosity tensor assumes the special form $\widehat{\mathbb{V}}_{IKV} = \zeta \, \hat{\mathbf{I}} \otimes \hat{\mathbf{I}} + 2\eta \, \widehat{\mathbb{P}} = (\zeta - \frac{2}{3}\eta) \, \hat{\mathbf{I}} \otimes \hat{\mathbf{I}} + 2\eta \, \widehat{\mathbb{I}}$, depending on two constant parameters: *bulk viscosity* ζ and *shear viscosity* η.

To compute the strain rate $\partial_t \hat{\mathbf{E}}'$ we use the expression (16) for the modified Green–Lagrange strain tensor of a Cosserat rod including the small strain approximation (12), with the result

$$\partial_t \hat{\mathbf{E}}' \approx \frac{1}{2} \left[\partial_t \mathbf{H} \otimes \mathbf{a}_0^{(3)} + \mathbf{a}_0^{(3)} \otimes \partial_t \mathbf{H} \right] - \nu \, \partial_t H_3 \left[\hat{\mathbf{I}} - \mathbf{a}_0^{(3)} \otimes \mathbf{a}_0^{(3)} \right] \tag{19}$$

depending on the time derivative $\partial_t \mathbf{H} = \partial_t H_k \, \mathbf{a}_0^{(k)}$ of the material strain vector with components

$$\partial_t H_1 = \partial_t V_1(s,t) - \xi_2 \, \partial_t U_3(s,t) , \quad \partial_t H_2 = \partial_t V_2(s,t) + \xi_1 \, \partial_t U_3(s,t)$$
$$\partial_t H_3 = \partial_t V_3(s,t) + \xi_2 \, \partial_t U_1(s,t) - \xi_1 \, \partial_t U_2(s,t) . \tag{20}$$

Inserting (19) and (20) into the dissipation density function $\Psi_{IKV}(\partial_t \hat{\mathbf{E}}) = \frac{1}{2} \partial_t \hat{\mathbf{E}} : \widehat{\mathbb{V}}_{IKV} : \partial_t \hat{\mathbf{E}}$ of the isotropic Kelvin–Voigt model, analogous computational steps as those done for the derivation of the stored energy $\Psi_{SVK}(\hat{\mathbf{E}}')$ in the previous subsection yield the expression

$$2\Psi_{IKV}(\partial_t \hat{\mathbf{E}}) \approx \left[\zeta(1-2\nu)^2 + \frac{4}{3}\eta(1+\nu)^2 \right] (\partial_t H_3)^2 + \eta \left[(\partial_t H_1)^2 + (\partial_t H_2)^2 \right] ,$$

with the *extensional viscosity* parameter η_E defined in (3) appearing as the prefactor of $(\partial_t H_3)^2$. The computation of the cross section integrals of the squared time derivatives $(\partial_t H_k)^2$ yields

$$\left\langle (\partial_t H_3)^2 \right\rangle_{\mathcal{A}} = A(\partial_t V_3)^2 + I_\alpha(\partial_t U_\alpha)^2 , \quad \left\langle (\partial_t H_1)^2 + (\partial_t H_2)^2 \right\rangle_{\mathcal{A}} = A\left[(\partial_t V_1)^2 + (\partial_t V_2)^2 \right] + I_3(\partial_t U_3)^2 ,$$

from which we obtain the desired cross section integral of the dissipation density function:

$$2\left\langle \Psi_{IKV}(\partial_t \hat{\mathbf{E}}) \right\rangle_{\mathcal{A}} \approx \eta_E A\,(\partial_t V_3)^2 + \eta_E I_\alpha\,(\partial_t U_\alpha)^2 + \eta A\left[(\partial_t V_1)^2 + (\partial_t V_2)^2 \right] + \eta I_3\,(\partial_t U_3)^2 . \quad (21)$$

The dissipation function (6) of the Cosserat rod with diagonal damping coefficient matrices (2) and damping parameters (3) is finally obtained as $W_{visc} = \int_0^L ds \left\langle \Psi_{IKV}(\partial_t \hat{\mathbf{E}}') \right\rangle_{\mathcal{A}}$ after introducing the shear correction factors (i.e.: $\eta A \to \eta A \kappa_\alpha$). This completes our derivation.

Kelvin–Voigt damping model for geometrically nonlinear ANCF beams
In the recent article [1], a damping model for geometrically nonlinear beams given in the ANCF (absolute nodal coordinates) formulation has been proposed. The authors obtained their model by inserting the 3D isotropic Kelvin–Voigt model as described above into their ANCF element ansatz. They used the Lamé parameters λ and μ as elastic moduli, and introduced corresponding viscosity parameters λ_v and μ_v, which they related to the elastic moduli by *dissipation factors* γ_{v1} and γ_{v2}. From the context it seems clear that in our notation $\gamma_{v2} = \tau_S$, such that $\mu_v = G\tau_S = \eta$. Likewise we may identify $\gamma_{v1} = \tau_B$, such that $\lambda_v = K\tau_B - \frac{2}{3}G\tau_S = \zeta - \frac{2}{3}\eta$, and the viscosities are related by the same relation as the elastic moduli (i.e.: $\lambda = K - \frac{2}{3}G$). As in our understanding the ANCF ansatz handles lateral contraction effects, both models should behave similar, with similar simulation results. However, a detailed comparison remains to be done.

Validity of the Kelvin–Voigt model
As remarked already in [6], the modelling of viscous dissipation for solids by a dissipation function of Kelvin–Voigt type is valid only for relatively slow processes near thermodynamic equilibrium, which means that the temperature within the solid should be approximately constant, and the macroscopic velocities of the material particles of the solid should be sufficiently slow w.r.t. the time scale of all internal relaxation processes. To illustrate this statement, we briefly discuss the one–dimensional example of a linear viscoelastic stress–strain relation $\sigma(t) = \int_0^\infty d\tau\, G(\tau)\dot{\varepsilon}(t-\tau)$ governed by the relaxation function $G(\tau) = G_\infty + \sum_{j=1}^N G_j \exp(-\tau/\tau_j)$ (i.e.: a *Prony series*) of a *generalized Maxwell model*. By Fourier transformation we obtain the relation $\hat{\sigma}(\omega) = \hat{G}(\omega)\hat{\varepsilon}(\omega)$ in the frequency domain, where the real and imaginary parts of the complex modulus function $\hat{G}(\omega) = G_\infty + \sum_{j=1}^N G_j \frac{i\tau_j\omega}{1+i\tau_j\omega}$ model the frequency dependent stiffness and damping properties of the material. Using a 1D Kelvin–Voigt model $\sigma_{KV}(t) = G\varepsilon(t) + \eta\dot{\varepsilon}(t)$ we obtain the simple expression $\hat{\sigma}_{KV}(\omega) = [G + i\eta\omega]\hat{\varepsilon}(\omega)$, which approximates the generalized Maxwell model at sufficiently low frequencies with $G = G_\infty$ and $\eta = \sum_{j=1}^N G_j\tau_j$. The deviation between the generalized Maxwell model and its Kelvin–Voigt approximation may be estimated as $|\sigma(t) - \sigma_{KV}(t)| \leq \frac{1}{2\pi} \int_{-\infty}^\infty d\omega\, |\hat{\varepsilon}(\omega)| \sum_{j=1}^N G_j \frac{(\tau_j\omega)^2}{\sqrt{1+(\tau_j\omega)^2}}$, which may indeed become small, provided that the strain spectrum $\hat{\varepsilon}(\omega)$ contains only frequencies much smaller than the inverse relaxation times $1/\tau_j$.

3 NUMERICAL EXAMPLE

To illustrate the behaviour of our damping model, we show the results of a numerical simulation of nonlinear vibrations of a cantilver beam in Fig. 1 obtained with the discrete Cosserat rod model presented in [7]. The beam is fully clamped at one end, the other end is pulled sideways far beyond the linear deformation range and then released. No gravitation is present. The parameters of the beam are: length $L = 0.3m$, quadratic cross-section area $A = 0.01 \times 0.01 m^2$, density $\rho = 10^3 kg/m^3$, Young's modulus $E = 10^6 Pa$, Poisson's ratio $\nu = 0.3$. The tests were performed with three different values of $\tau_E = \tau_{B/S} = 0.01s,\ 0.02s,\ 0.04s$.
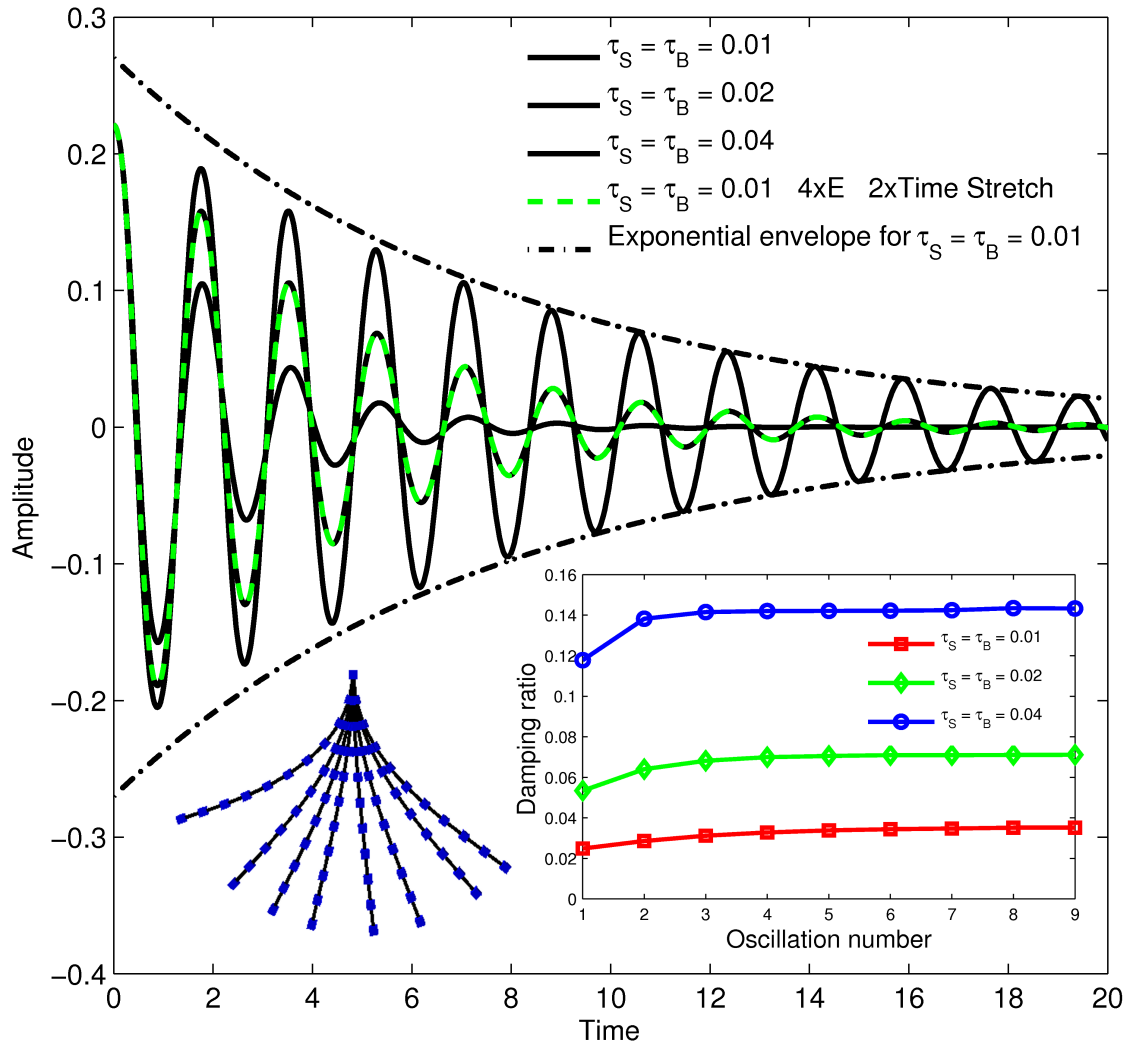
Figure 1. Damped non-linear bending vibrations of a clamped cantilever beam.

The deformations of the beam shown in the inset of Fig. 1 are snapshots taken during the first period of the oscillations which illustrate that in the initial phase of the oscillations substantial geometric nonlinearities are present. During the vibrations the beam remains in the plane of its initial deformation, such that all deformations are of plane bending type, and the extensional viscosity $\eta_E = E\tau_E$ becomes the main damping factor. As expected, the plots of the transverse oscillation amplitude $x(t) = \mathbf{e}_1 \cdot \boldsymbol{\varphi}(L, t)$ recorded at the free end of the beam show an exponential dying out in the range of small amplitudes (linear regime). The deviations from the exponential envelope adapted to the linear regime that are observed during the initial phase clearly show the influence of geometric nonlinearity. The plots also suggest that damping becomes weaker in the nonlinear range. However, linear behaviour seems to start already with the fifth oscillation period, where the amplitude still has a large value of $\approx L/3$.

This may be further analyzed by evaluating the *logarithmic decrements* $\delta_k = \ln(x(t_k)/x(t_{k+1}))$ recorded between succesive maxima $x(t_k)$ of the amplitude as well as the corresponding *damping ratios* ζ_k implicitly defined [4] by $\delta_k = 2\pi\zeta_k/\sqrt{1 - \zeta_k^2}$. The plots for the values of ζ_k determined in this way are shown in the inset of Fig. 1. As expected, the ratios approach constant values in the linear regime, which scale as $1 : 2 : 4$ proportional to the values of the time constant τ_E used in the simulations. The simulations also show that the decrements become lower in the range of large amplitudes, which confirms the observation that the damping effect of our Kelvin–Voigt model is extenuated by the presence of geometrical nonlinearity. Nevertheless, ζ_k still scales approximately proportional to τ_E also in the nonlinear range.

To investigate the influence of a variation of the bending stiffness on the damping behaviour, an additional test with quadrupled Young's modulus $E = 4 \cdot 10^6$ was performed. In the corresponding amplitude plot shown in Fig. 1 the time axis of the plot with quadrupled E was streched twofold, such that the oscillations could be compared directly. After time stretching the $(E = 4 \cdot 10^6, \tau_E = 0.01)$ plot coincides with the $(E = 10^6, \tau_E = 0.02)$ plot, surprisingly even throughout the whole nonlinear range. Since the oscillation period T of the $E = 4 \cdot 10^6$ beam is two times smaller than that of the $E = 10^6$ beam, this suggests that the damping ratio varies proportional to the ratio τ_E/T. Again this would be the expected behaviour in the linear regime, but is observed here in the nonlinear range as well.

4 CONCLUSION

In our paper we presented the derivation of a viscous Kelvin–Voigt type damping model for geometrically exact Cosserat rods. For homogeneous and isotropic materials we computed the damping parameters explicitly in terms of the stiffness parameters and retardation time constants. In numerical simulations of vibrations of a clamped cantilever beam we observed a weakening influence of geometric nonlinearities on the damping of the oscillation amplitudes. We also found that the variation of retardation time and bending stiffness has a similar effect on the damping ratio as in the linear regime. In view of the limitations of the Kelvin–Voigt model w.r.t. higher frequencies it would be worthwile to develop more complex viscoelastic models (e.g. of generalized Maxwell type) for Cosserat rods. The technical details of our derivation of the Kelvin–Voigt model may be helpful to derive such models from 3D continuum theory in an analogous way.

REFERENCES

[1] Abdel–Nasser, A.M.; Shabana, A.A.: A nonlinear visco–elastic constitutive model for large rotation finite element formulations. Multibody System Dynamics, Vol. 26, No. 3, pp. 57–79, 2011.

[2] Antman, S.S.: Invariant dissipative mechanisms for the spatial motion of rods suggested by artificial viscosity. Journal of Elasticity, Vol. 70, pp. 55–64, 2003.

[3] Antman, S.S.: Nonlinear Problems of Elasticity (2nd Edition). Springer, 2005.

[4] Craig, R.R. and Kurdila, A.J.: Fundamentals of Structural Dynamics (2nd Edition). John Wiley & Sons, 2006.

[5] Géradin, M.; Cardona, A.: Flexible Multibody Dynamics: A Finite Element Approach. John Wiley & Sons, 2001.

[6] Landau, L.D.; Lifshitz, E.M.: Theory of Elasticity (Course of Theoretical Physics Vol. 7, 3rd ed.). Butterworth Heinemann, 1986.

[7] Lang, H.; Linn, J.; Arnold, M.: Multibody dynamics simulation of geometrically exact Cosserat Rods. Multibody System Dynamics, Vol. 25, No. 3, pp. 285–312, 2011. Extended version: Berichte des ITWM, Nr. **209**, 2011.

[8] Lemaitre, J.; Chaboche, J.-L.: Mechanics of Solid Materials. Cambridge Universtity Press, 1990.

[9] Love, A.E.H.: A Treatise on the Mathematical Theory of Elasticity. 4th edition (1927), reprinted by Dover, New York, 1963.

[10] Simo, J.C.: A finite strain beam formulation: the three dimensional dynamic problem – Part I. Comp. Meth. Apl. Mech. Engrg., Vol. 49, pp. 55–70, 1985.

[11] Weiss, H.: Dynamics of Geometrically Nonlinear Rods: I — Mechanical Models and Equations of Motion. Nonlinear Dynamics, Vol. 30, pp. 357–381, 2002.

Published reports of the Fraunhofer ITWM

The PDF-files of the following reports are available under:
www.itwm.fraunhofer.de/de/ zentral__berichte/berichte

34. I. Ginzburg, K. Steiner

Lattice Boltzmann Model for Free-Surface flow and Its Application to Filling Process in Casting

Keywords: Lattice Boltzmann models; free-surface phenomena; interface boundary conditions; filling processes; injection molding; volume of fluid method; interface boundary conditions; advection-schemes; upwind-schemes

(54 pages, 2002)

35. M. Günther, A. Klar, T. Materne, R. Wegener

Multivalued fundamental diagrams and stop and go waves for continuum traffic equations

Keywords: traffic flow, macroscopic equations, kinetic derivation, multivalued fundamental diagram, stop and go waves, phase transitions

(25 pages, 2002)

36. S. Feldmann, P. Lang, D. Prätzel-Wolters

Parameter influence on the zeros of network determinants

Keywords: Networks, Equicofactor matrix polynomials, Realization theory, Matrix perturbation theory

(30 pages, 2002)

37. K. Koch, J. Ohser, K. Schladitz

Spectral theory for random closed sets and estimating the covariance via frequency space

Keywords: Random set, Bartlett spectrum, fast Fourier transform, power spectrum

(28 pages, 2002)

38. D. d'Humières, I. Ginzburg

Multi-reflection boundary conditions for lattice Boltzmann models

Keywords: lattice Boltzmann equation, boudary conditions, bounce-back rule, Navier-Stokes equation

(72 pages, 2002)

39. R. Korn

Elementare Finanzmathematik

Keywords: Finanzmathematik, Aktien, Optionen, Portfolio-Optimierung, Börse, Lehrerweiterbildung, Mathematikunterricht

(98 pages, 2002)

40. J. Kallrath, M. C. Müller, S. Nickel

Batch Presorting Problems: Models and Complexity Results

Keywords: Complexity theory, Integer programming, Assigment, Logistics

(19 pages, 2002)

41. J. Linn

On the frame-invariant description of the phase space of the Folgar-Tucker equation

Key words: fiber orientation, Folgar-Tucker equation, injection molding

(5 pages, 2003)

42. T. Hanne, S. Nickel

A Multi-Objective Evolutionary Algorithm for Scheduling and Inspection Planning in Software Development Projects

Key words: multiple objective programming, project management and scheduling, software development, evolutionary algorithms, efficient set

(29 pages, 2003)

43. T. Bortfeld , K.-H. Küfer, M. Monz, A. Scherrer, C. Thieke, H. Trinkaus

Intensity-Modulated Radiotherapy - A Large Scale Multi-Criteria Programming Problem

Keywords: multiple criteria optimization, representative systems of Pareto solutions, adaptive triangulation, clustering and disaggregation techniques, visualization of Pareto solutions, medical physics, external beam radiotherapy planning, intensity modulated radiotherapy

(31 pages, 2003)

44. T. Halfmann, T. Wichmann

Overview of Symbolic Methods in Industrial Analog Circuit Design

Keywords: CAD, automated analog circuit design, symbolic analysis, computer algebra, behavioral modeling, system simulation, circuit sizing, macro modeling, differential-algebraic equations, index

(17 pages, 2003)

45. S. E. Mikhailov, J. Orlik

Asymptotic Homogenisation in Strength and Fatigue Durability Analysis of Composites

Keywords: multiscale structures, asymptotic homogenization, strength, fatigue, singularity, non-local conditions

(14 pages, 2003)

46. P. Domínguez-Marín, P. Hansen, N. Mladenovic , S. Nickel

Heuristic Procedures for Solving the Discrete Ordered Median Problem

Keywords: genetic algorithms, variable neighborhood search, discrete facility location

(31 pages, 2003)

47. N. Boland, P. Domínguez-Marín, S. Nickel, J. Puerto

Exact Procedures for Solving the Discrete Ordered Median Problem

Keywords: discrete location, Integer programming

(41 pages, 2003)

48. S. Feldmann, P. Lang

Padé-like reduction of stable discrete linear systems preserving their stability

Keywords: Discrete linear systems, model reduction, stability, Hankel matrix, Stein equation

(16 pages, 2003)

49. J. Kallrath, S. Nickel

A Polynomial Case of the Batch Presorting Problem

Keywords: batch presorting problem, online optimization, competetive analysis, polynomial algorithms, logistics

(17 pages, 2003)

50. T. Hanne, H. L. Trinkaus

knowCube for MCDM – Visual and Interactive Support for Multicriteria Decision Making

Key words: Multicriteria decision making, knowledge management, decision support systems, visual interfaces, interactive navigation, real-life applications.

(26 pages, 2003)

51. O. Iliev, V. Laptev

On Numerical Simulation of Flow Through Oil Filters

Keywords: oil filters, coupled flow in plain and porous media, Navier-Stokes, Brinkman, numerical simulation

(8 pages, 2003)

52. W. Dörfler, O. Iliev, D. Stoyanov, D. Vassileva

On a Multigrid Adaptive Refinement Solver for Saturated Non-Newtonian Flow in Porous Media

Keywords: Nonlinear multigrid, adaptive refinement, non-Newtonian flow in porous media

(17 pages, 2003)

53. S. Kruse

On the Pricing of Forward Starting Options under Stochastic Volatility

Keywords: Option pricing, forward starting options, Heston model, stochastic volatility, cliquet options

(11 pages, 2003)

54. O. Iliev, D. Stoyanov

Multigrid – adaptive local refinement solver for incompressible flows

Keywords: Navier-Stokes equations, incompressible flow, projection-type splitting, SIMPLE, multigrid methods, adaptive local refinement, lid-driven flow in a cavity

(37 pages, 2003)

55. V. Starikovicius

The multiphase flow and heat transfer in porous media

Keywords: Two-phase flow in porous media, various formulations, global pressure, multiphase mixture model, numerical simulation

(30 pages, 2003)

56. P. Lang, A. Sarishvili, A. Wirsen

Blocked neural networks for knowledge extraction in the software development process

Keywords: Blocked Neural Networks, Nonlinear Regression, Knowledge Extraction, Code Inspection

(21 pages, 2003)

57. H. Knaf, P. Lang, S. Zeiser

Diagnosis aiding in Regulation Thermography using Fuzzy Logic

Keywords: fuzzy logic,knowledge representation, expert system

(22 pages, 2003)

58. M. T. Melo, S. Nickel, F. Saldanha da Gama

Largescale models for dynamic multicommodity capacitated facility location

Keywords: supply chain management, strategic planning, dynamic location, modeling

(40 pages, 2003)

59. J. Orlik

Homogenization for contact problems with periodically rough surfaces

Keywords: asymptotic homogenization, contact problems

(28 pages, 2004)

60. A. Scherrer, K.-H. Küfer, M. Monz, F. Alonso, T. Bortfeld

IMRT planning on adaptive volume structures – a significant advance of computational complexity

Keywords: Intensity-modulated radiation therapy (IMRT), inverse treatment planning, adaptive volume structures, hierarchical clustering, local refinement, adaptive clustering, convex programming, mesh generation, multi-grid methods

(24 pages, 2004)

61. D. Kehrwald

Parallel lattice Boltzmann simulation of complex flows

Keywords: Lattice Boltzmann methods, parallel computing, microstructure simulation, virtual material design, pseudo-plastic fluids, liquid composite moulding

(12 pages, 2004)

62. O. Iliev, J. Linn, M. Moog, D. Niedziela, V. Starikovicius

On the Performance of Certain Iterative Solvers for Coupled Systems Arising in Discretization of Non-Newtonian Flow Equations

Keywords: Performance of iterative solvers, Preconditioners, Non-Newtonian flow
(17 pages, 2004)

63. R. Ciegis, O. Iliev, S. Rief, K. Steiner
On Modelling and Simulation of Different Regimes for Liquid Polymer Moulding
Keywords: Liquid Polymer Moulding, Modelling, Simulation, Infiltration, Front Propagation, non-Newtonian flow in porous media
(43 pages, 2004)

64. T. Hanne, H. Neu
Simulating Human Resources in Software Development Processes
Keywords: Human resource modeling, software process, productivity, human factors, learning curve
(14 pages, 2004)

65. O. Iliev, A. Mikelic, P. Popov
Fluid structure interaction problems in deformable porous media: Toward permeability of deformable porous media
Keywords: fluid-structure interaction, deformable porous media, upscaling, linear elasticity, stokes, finite elements
(28 pages, 2004)

66. F. Gaspar, O. Iliev, F. Lisbona, A. Naumovich, P. Vabishchevich
On numerical solution of 1-D poroelasticity equations in a multilayered domain
Keywords: poroelasticity, multilayered material, finite volume discretization, MAC type grid
(41 pages, 2004)

67. J. Ohser, K. Schladitz, K. Koch, M. Nöthe
Diffraction by image processing and its application in materials science
Keywords: porous microstructure, image analysis, random set, fast Fourier transform, power spectrum, Bartlett spectrum
(13 pages, 2004)

68. H. Neunzert
Mathematics as a Technology: Challenges for the next 10 Years
Keywords: applied mathematics, technology, modelling, simulation, visualization, optimization, glass processing, spinning processes, fiber-fluid interaction, trubulence effects, topological optimization, multicriteria optimization, Uncertainty and Risk, financial mathematics, Malliavin calculus, Monte-Carlo methods, virtual material design, filtration, bio-informatics, system biology
(29 pages, 2004)

69. R. Ewing, O. Iliev, R. Lazarov, A. Naumovich
On convergence of certain finite difference discretizations for 1D poroelasticity interface problems
Keywords: poroelasticity, multilayered material, finite volume discretizations, MAC type grid, error estimates
(26 pages,2004)

70. W. Dörfler, O. Iliev, D. Stoyanov, D. Vassileva
On Efficient Simulation of Non-Newtonian Flow in Saturated Porous Media with a Multigrid Adaptive Refinement Solver
Keywords: Nonlinear multigrid, adaptive renement, non-Newtonian in porous media
(25 pages, 2004)

71. J. Kalcsics, S. Nickel, M. Schröder
Towards a Unified Territory Design Approach – Applications, Algorithms and GIS Integration
Keywords: territory desgin, political districting, sales territory alignment, optimization algorithms, Geographical Information Systems
(40 pages, 2005)

72. K. Schladitz, S. Peters, D. Reinel-Bitzer, A. Wiegmann, J. Ohser
Design of acoustic trim based on geometric modeling and flow simulation for non-woven
Keywords: random system of fibers, Poisson line process, flow resistivity, acoustic absorption, Lattice-Boltzmann method, non-woven
(21 pages, 2005)

73. V. Rutka, A. Wiegmann
Explicit Jump Immersed Interface Method for virtual material design of the effective elastic moduli of composite materials
Keywords: virtual material design, explicit jump immersed interface method, effective elastic moduli, composite materials
(22 pages, 2005)

74. T. Hanne
Eine Übersicht zum Scheduling von Baustellen
Keywords: Projektplanung, Scheduling, Bauplanung, Bauindustrie
(32 pages, 2005)

75. J. Linn
The Folgar-Tucker Model as a Differetial Algebraic System for Fiber Orientation Calculation
Keywords: fiber orientation, Folgar–Tucker model, invariants, algebraic constraints, phase space, trace stability
(15 pages, 2005)

76. M. Speckert, K. Dreßler, H. Mauch, A. Lion, G. J. Wierda
Simulation eines neuartigen Prüfsystems für Achserprobungen durch MKS-Modellierung einschließlich Regelung
Keywords: virtual test rig, suspension testing, multibody simulation, modeling hexapod test rig, optimization of test rig configuration
(20 pages, 2005)

77. K.-H. Küfer, M. Monz, A. Scherrer, P. Süss, F. Alonso, A.S.A. Sultan, Th. Bortfeld, D. Craft, Chr. Thieke
Multicriteria optimization in intensity modulated radiotherapy planning
Keywords: multicriteria optimization, extreme solutions, real-time decision making, adaptive approximation schemes, clustering methods, IMRT planning, reverse engineering
(51 pages, 2005)

78. S. Amstutz, H. Andrä
A new algorithm for topology optimization using a level-set method
Keywords: shape optimization, topology optimization, topological sensitivity, level-set
(22 pages, 2005)

79. N. Ettrich
Generation of surface elevation models for urban drainage simulation
Keywords: Flooding, simulation, urban elevation models, laser scanning
(22 pages, 2005)

80. H. Andrä, J. Linn, I. Matei, I. Shklyar, K. Steiner, E. Teichmann
OPTCAST – Entwicklung adäquater Strukturoptimierungsverfahren für Gießereien Technischer Bericht (KURZFASSUNG)
Keywords: Topologieoptimierung, Level-Set-Methode, Gießprozesssimulation, Gießtechnische Restriktionen, CAE-Kette zur Strukturoptimierung
(77 pages, 2005)

81. N. Marheineke, R. Wegener
**Fiber Dynamics in Turbulent Flows
Part I: General Modeling Framework**
Keywords: fiber-fluid interaction; Cosserat rod; turbulence modeling; Kolmogorov's energy spectrum; double-velocity correlations; differentiable Gaussian fields
(20 pages, 2005)

Part II: Specific Taylor Drag
Keywords: flexible fibers; k-ε turbulence model; fiber-turbulence interaction scales; air drag; random Gaussian aerodynamic force; white noise; stochastic differential equations; ARMA process
(18 pages, 2005)

82. C. H. Lampert, O. Wirjadi
An Optimal Non-Orthogonal Separation of the Anisotropic Gaussian Convolution Filter
Keywords: Anisotropic Gaussian filter, linear filtering, orientation space, nD image processing, separable filters
(25 pages, 2005)

83. H. Andrä, D. Stoyanov
Error indicators in the parallel finite element solver for linear elasticity DDFEM
Keywords: linear elasticity, finite element method, hierarchical shape functions, domain decom-position, parallel implementation, a posteriori error estimates
(21 pages, 2006)

84. M. Schröder, I. Solchenbach
Optimization of Transfer Quality in Regional Public Transit
Keywords: public transit, transfer quality, quadratic assignment problem
(16 pages, 2006)

85. A. Naumovich, F. J. Gaspar
On a multigrid solver for the three-dimensional Biot poroelasticity system in multilayered domains
Keywords: poroelasticity, interface problem, multigrid, operator-dependent prolongation
(11 pages, 2006)

86. S. Panda, R. Wegener, N. Marheineke
Slender Body Theory for the Dynamics of Curved Viscous Fibers
Keywords: curved viscous fibers; fluid dynamics; Navier-Stokes equations; free boundary value problem; asymptotic expansions; slender body theory
(14 pages, 2006)

87. E. Ivanov, H. Andrä, A. Kudryavtsev
Domain Decomposition Approach for Automatic Parallel Generation of Tetrahedral Grids
Key words: Grid Generation, Unstructured Grid, Delaunay Triangulation, Parallel Programming, Domain Decomposition, Load Balancing
(18 pages, 2006)

88. S. Tiwari, S. Antonov, D. Hietel, J. Kuhnert, R. Wegener
A Meshfree Method for Simulations of Interactions between Fluids and Flexible Structures
Key words: Meshfree Method, FPM, Fluid Structure Interaction, Sheet of Paper, Dynamical Coupling
(16 pages, 2006)

89. R. Ciegis , O. Iliev, V. Starikovicius, K. Steiner
Numerical Algorithms for Solving Problems of Multiphase Flows in Porous Media
Keywords: nonlinear algorithms, finite-volume method, software tools, porous media, flows
(16 pages, 2006)

90. D. Niedziela, O. Iliev, A. Latz

On 3D Numerical Simulations of Viscoelastic Fluids

Keywords: non-Newtonian fluids, anisotropic viscosity, integral constitutive equation

(18 pages, 2006)

91. A. Winterfeld

Application of general semi-infinite Programming to Lapidary Cutting Problems

Keywords: large scale optimization, nonlinear programming, general semi-infinite optimization, design centering, clustering

(26 pages, 2006)

92. J. Orlik, A. Ostrovska

Space-Time Finite Element Approximation and Numerical Solution of Hereditary Linear Viscoelasticity Problems

Keywords: hereditary viscoelasticity; kern approximation by interpolation; space-time finite element approximation, stability and a priori estimate

(24 pages, 2006)

93. V. Rutka, A. Wiegmann, H. Andrä

EJIIM for Calculation of effective Elastic Moduli in 3D Linear Elasticity

Keywords: Elliptic PDE, linear elasticity, irregular domain, finite differences, fast solvers, effective elastic moduli

(24 pages, 2006)

94. A. Wiegmann, A. Zemitis

EJ-HEAT: A Fast Explicit Jump Harmonic Averaging Solver for the Effective Heat Conductivity of Composite Materials

Keywords: Stationary heat equation, effective thermal conductivity, explicit jump, discontinuous coefficients, virtual material design, microstructure simulation, EJ-HEAT

(21 pages, 2006)

95. A. Naumovich

On a finite volume discretization of the three-dimensional Biot poroelasticity system in multilayered domains

Keywords: Biot poroelasticity system, interface problems, finite volume discretization, finite difference method

(21 pages, 2006)

96. M. Krekel, J. Wenzel

A unified approach to Credit Default Swaption and Constant Maturity Credit Default Swap valuation

Keywords: LIBOR market model, credit risk, Credit Default Swaption, Constant Maturity Credit Default Swapmethod

(43 pages, 2006)

97. A. Dreyer

Interval Methods for Analog Circiuts

Keywords: interval arithmetic, analog circuits, tolerance analysis, parametric linear systems, frequency response, symbolic analysis, CAD, computer algebra

(36 pages, 2006)

98. N. Weigel, S. Weihe, G. Bitsch, K. Dreßler

Usage of Simulation for Design and Optimization of Testing

Keywords: Vehicle test rigs, MBS, control, hydraulics, testing philosophy

(14 pages, 2006)

99. H. Lang, G. Bitsch, K. Dreßler, M. Speckert

Comparison of the solutions of the elastic and elastoplastic boundary value problems

Keywords: Elastic BVP, elastoplastic BVP, variational inequalities, rate-independency, hysteresis, linear kinematic hardening, stop- and play-operator

(21 pages, 2006)

100. M. Speckert, K. Dreßler, H. Mauch

MBS Simulation of a hexapod based suspension test rig

Keywords: Test rig, MBS simulation, suspension, hydraulics, controlling, design optimization

(12 pages, 2006)

101. S. Azizi Sultan, K.-H. Küfer

A dynamic algorithm for beam orientations in multicriteria IMRT planning

Keywords: radiotherapy planning, beam orientation optimization, dynamic approach, evolutionary algorithm, global optimization

(14 pages, 2006)

102. T. Götz, A. Klar, N. Marheineke, R. Wegener

A Stochastic Model for the Fiber Lay-down Process in the Nonwoven Production

Keywords: fiber dynamics, stochastic Hamiltonian system, stochastic averaging

(17 pages, 2006)

103. Ph. Süss, K.-H. Küfer

Balancing control and simplicity: a variable aggregation method in intensity modulated radiation therapy planning

Keywords: IMRT planning, variable aggregation, clustering methods

(22 pages, 2006)

104. A. Beaudry, G. Laporte, T. Melo, S. Nickel

Dynamic transportation of patients in hospitals

Keywords: in-house hospital transportation, dial-a-ride, dynamic mode, tabu search

(37 pages, 2006)

105. Th. Hanne

Applying multiobjective evolutionary algorithms in industrial projects

Keywords: multiobjective evolutionary algorithms, discrete optimization, continuous optimization, electronic circuit design, semi-infinite programming, scheduling

(18 pages, 2006)

106. J. Franke, S. Halim

Wild bootstrap tests for comparing signals and images

Keywords: wild bootstrap test, texture classification, textile quality control, defect detection, kernel estimate, nonparametric regression

(13 pages, 2007)

107. Z. Drezner, S. Nickel

Solving the ordered one-median problem in the plane

Keywords: planar location, global optimization, ordered median, big triangle small triangle method, bounds, numerical experiments

(21 pages, 2007)

108. Th. Götz, A. Klar, A. Unterreiter, R. Wegener

Numerical evidence for the non-existing of solutions of the equations desribing rotational fiber spinning

Keywords: rotational fiber spinning, viscous fibers, boundary value problem, existence of solutions

(11 pages, 2007)

109. Ph. Süss, K.-H. Küfer

Smooth intensity maps and the Bortfeld-Boyer sequencer

Keywords: probabilistic analysis, intensity modulated radiotherapy treatment (IMRT), IMRT plan application, step-and-shoot sequencing

(8 pages, 2007)

110. E. Ivanov, O. Gluchshenko, H. Andrä, A. Kudryavtsev

Parallel software tool for decomposing and meshing of 3d structures

Keywords: a-priori domain decomposition, unstructured grid, Delaunay mesh generation

(14 pages, 2007)

111. O. Iliev, R. Lazarov, J. Willems

Numerical study of two-grid preconditioners for 1d elliptic problems with highly oscillating discontinuous coefficients

Keywords: two-grid algorithm, oscillating coefficients, preconditioner

(20 pages, 2007)

112. L. Bonilla, T. Götz, A. Klar, N. Marheineke, R. Wegener

Hydrodynamic limit of the Fokker-Planck-equation describing fiber lay-down processes

Keywords: stochastic dierential equations, Fokker-Planck equation, asymptotic expansion, Ornstein-Uhlenbeck process

(17 pages, 2007)

113. S. Rief

Modeling and simulation of the pressing section of a paper machine

Keywords: paper machine, computational fluid dynamics, porous media

(41 pages, 2007)

114. R. Ciegis, O. Iliev, Z. Lakdawala

On parallel numerical algorithms for simulating industrial filtration problems

Keywords: Navier-Stokes-Brinkmann equations, finite volume discretization method, SIMPLE, parallel computing, data decomposition method

(24 pages, 2007)

115. N. Marheineke, R. Wegener

Dynamics of curved viscous fibers with surface tension

Keywords: Slender body theory, curved viscous bers with surface tension, free boundary value problem

(25 pages, 2007)

116. S. Feth, J. Franke, M. Speckert

Resampling-Methoden zur mse-Korrektur und Anwendungen in der Betriebsfestigkeit

Keywords: Weibull, Bootstrap, Maximum-Likelihood, Betriebsfestigkeit

(16 pages, 2007)

117. H. Knaf

Kernel Fisher discriminant functions – a concise and rigorous introduction

Keywords: wild bootstrap test, texture classification, textile quality control, defect detection, kernel estimate, nonparametric regression

(30 pages, 2007)

118. O. Iliev, I. Rybak

On numerical upscaling for flows in heterogeneous porous media

Keywords: numerical upscaling, heterogeneous porous media, single phase flow, Darcy's law, multiscale problem, effective permeability, multipoint flux approximation, anisotropy
(17 pages, 2007)

119. O. Iliev, I. Rybak

On approximation property of multipoint flux approximation method

Keywords: Multipoint flux approximation, finite volume method, elliptic equation, discontinuous tensor coefficients, anisotropy
(15 pages, 2007)

120. O. Iliev, I. Rybak, J. Willems

On upscaling heat conductivity for a class of industrial problems

Keywords: Multiscale problems, effective heat conductivity, numerical upscaling, domain decomposition
(21 pages, 2007)

121. R. Ewing, O. Iliev, R. Lazarov, I. Rybak

On two-level preconditioners for flow in porous media

Keywords: Multiscale problem, Darcy's law, single phase flow, anisotropic heterogeneous porous media, numerical upscaling, multigrid, domain decomposition, efficient preconditioner
(18 pages, 2007)

122. M. Brickenstein, A. Dreyer

POLYBORI: A Gröbner basis framework for Boolean polynomials

Keywords: Gröbner basis, formal verification, Boolean polynomials, algebraic cryptoanalysis, satisfiability
(23 pages, 2007)

123. O. Wirjadi

Survey of 3d image segmentation methods

Keywords: image processing, 3d, image segmentation, binarization
(20 pages, 2007)

124. S. Zeytun, A. Gupta

A Comparative Study of the Vasicek and the CIR Model of the Short Rate

Keywords: interest rates, Vasicek model, CIR-model, calibration, parameter estimation
(17 pages, 2007)

125. G. Hanselmann, A. Sarishvili

Heterogeneous redundancy in software quality prediction using a hybrid Bayesian approach

Keywords: reliability prediction, fault prediction, non-homogeneous poisson process, Bayesian model averaging
(17 pages, 2007)

126. V. Maag, M. Berger, A. Winterfeld, K.-H. Küfer

A novel non-linear approach to minimal area rectangular packing

Keywords: rectangular packing, non-overlapping constraints, non-linear optimization, regularization, relaxation
(18 pages, 2007)

127. M. Monz, K.-H. Küfer, T. Bortfeld, C. Thieke

Pareto navigation – systematic multi-criteria-based IMRT treatment plan determination

Keywords: convex, interactive multi-objective optimization, intensity modulated radiotherapy planning
(15 pages, 2007)

128. M. Krause, A. Scherrer

On the role of modeling parameters in IMRT plan optimization

Keywords: intensity-modulated radiotherapy (IMRT), inverse IMRT planning, convex optimization, sensitivity analysis, elasticity, modeling parameters, equivalent uniform dose (EUD)
(18 pages, 2007)

129. A. Wiegmann

Computation of the permeability of porous materials from their microstructure by FFF-Stokes

Keywords: permeability, numerical homogenization, fast Stokes solver
(24 pages, 2007)

130. T. Melo, S. Nickel, F. Saldanha da Gama

Facility Location and Supply Chain Management – A comprehensive review

Keywords: facility location, supply chain management, network design
(54 pages, 2007)

131. T. Hanne, T. Melo, S. Nickel

Bringing robustness to patient flow management through optimized patient transports in hospitals

Keywords: Dial-a-Ride problem, online problem, case study, tabu search, hospital logistics
(23 pages, 2007)

132. R. Ewing, O. Iliev, R. Lazarov, I. Rybak, J. Willems

An efficient approach for upscaling properties of composite materials with high contrast of coefficients

Keywords: effective heat conductivity, permeability of fractured porous media, numerical upscaling, fibrous insulation materials, metal foams
(16 pages, 2008)

133. S. Gelareh, S. Nickel

New approaches to hub location problems in public transport planning

Keywords: integer programming, hub location, transportation, decomposition, heuristic
(25 pages, 2008)

134. G. Thömmes, J. Becker, M. Junk, A. K. Vaikuntam, D. Kehrwald, A. Klar, K. Steiner, A. Wiegmann

A Lattice Boltzmann Method for immiscible multiphase flow simulations using the Level Set Method

Keywords: Lattice Boltzmann method, Level Set method, free surface, multiphase flow
(28 pages, 2008)

135. J. Orlik

Homogenization in elasto-plasticity

Keywords: multiscale structures, asymptotic homogenization, nonlinear energy
(40 pages, 2008)

136. J. Almquist, H. Schmidt, P. Lang, J. Deitmer, M. Jirstrand, D. Prätzel-Wolters, H. Becker

Determination of interaction between MCT1 and CAII via a mathematical and physiological approach

Keywords: mathematical modeling; model reduction; electrophysiology; pH-sensitive microelectrodes; proton antenna
(20 pages, 2008)

137. E. Savenkov, H. Andrä, O. Iliev

An analysis of one regularization approach for solution of pure Neumann problem

Keywords: pure Neumann problem, elasticity, regularization, finite element method, condition number
(27 pages, 2008)

138. O. Berman, J. Kalcsics, D. Krass, S. Nickel

The ordered gradual covering location problem on a network

Keywords: gradual covering, ordered median function, network location
(32 pages, 2008)

139. S. Gelareh, S. Nickel

Multi-period public transport design: A novel model and solution approaches

Keywords: Integer programming, hub location, public transport, multi-period planning, heuristics
(31 pages, 2008)

140. T. Melo, S. Nickel, F. Saldanha-da-Gama

Network design decisions in supply chain planning

Keywords: supply chain design, integer programming models, location models, heuristics
(20 pages, 2008)

141. C. Lautensack, A. Särkkä, J. Freitag, K. Schladitz

Anisotropy analysis of pressed point processes

Keywords: estimation of compression, isotropy test, nearest neighbour distance, orientation analysis, polar ice, Ripley's K function
(35 pages, 2008)

142. O. Iliev, R. Lazarov, J. Willems

A Graph-Laplacian approach for calculating the effective thermal conductivity of complicated fiber geometries

Keywords: graph laplacian, effective heat conductivity, numerical upscaling, fibrous materials
(14 pages, 2008)

143. J. Linn, T. Stephan, J. Carlsson, R. Bohlin

Fast simulation of quasistatic rod deformations for VR applications

Keywords: quasistatic deformations, geometrically exact rod models, variational formulation, energy minimization, finite differences, nonlinear conjugate gradients
(7 pages, 2008)

144. J. Linn, T. Stephan

Simulation of quasistatic deformations using discrete rod models

Keywords: quasistatic deformations, geometrically exact rod models, variational formulation, energy minimization, finite differences, nonlinear conjugate gradients
(9 pages, 2008)

145. J. Marburger, N. Marheineke, R. Pinnau

Adjoint based optimal control using mesh-less discretizations

Keywords: Mesh-less methods, particle methods, Eulerian-Lagrangian formulation, optimization strategies, adjoint method, hyperbolic equations
(14 pages, 2008

146. S. Desmettre, J. Gould, A. Szimayer

Own-company stockholding and work effort preferences of an unconstrained executive

Keywords: optimal portfolio choice, executive compensation
(33 pages, 2008)

147. M. Berger, M. Schröder, K.-H. Küfer
A constraint programming approach for the two-dimensional rectangular packing problem with orthogonal orientations
Keywords: rectangular packing, orthogonal orientations non-overlapping constraints, constraint propagation
(13 pages, 2008)

148. K. Schladitz, C. Redenbach, T. Sych, M. Godehardt
Microstructural characterisation of open foams using 3d images
Keywords: virtual material design, image analysis, open foams
(30 pages, 2008)

149. E. Fernández, J. Kalcsics, S. Nickel, R. Ríos-Mercado
A novel territory design model arising in the implementation of the WEEE-Directive
Keywords: heuristics, optimization, logistics, recycling
(28 pages, 2008)

150. H. Lang, J. Linn
Lagrangian field theory in space-time for geometrically exact Cosserat rods
Keywords: Cosserat rods, geometrically exact rods, small strain, large deformation, deformable bodies, Lagrangian field theory, variational calculus
(19 pages, 2009)

151. K. Dreßler, M. Speckert, R. Müller, Ch. Weber
Customer loads correlation in truck engineering
Keywords: Customer distribution, safety critical components, quantile estimation, Monte-Carlo methods
(11 pages, 2009)

152. H. Lang, K. Dreßler
An improved multiaxial stress-strain correction model for elastic FE postprocessing
Keywords: Jiang's model of elastoplasticity, stress-strain correction, parameter identification, automatic differentiation, least-squares optimization, Coleman-Li algorithm
(6 pages, 2009)

153. J. Kalcsics, S. Nickel, M. Schröder
A generic geometric approach to territory design and districting
Keywords: Territory design, districting, combinatorial optimization, heuristics, computational geometry
(32 pages, 2009)

154. Th. Fütterer, A. Klar, R. Wegener
An energy conserving numerical scheme for the dynamics of hyperelastic rods
Keywords: Cosserat rod, hyperealstic, energy conservation, finite differences
(16 pages, 2009)

155. A. Wiegmann, L. Cheng, E. Glatt, O. Iliev, S. Rief
Design of pleated filters by computer simulations
Keywords: Solid-gas separation, solid-liquid separation, pleated filter, design, simulation
(21 pages, 2009)

156. A. Klar, N. Marheineke, R. Wegener
Hierarchy of mathematical models for production processes of technical textiles
Keywords: Fiber-fluid interaction, slender-body theory, turbulence modeling, model reduction, stochastic differential equations, Fokker-Planck equation, asymptotic expansions, parameter identification
(21 pages, 2009)

157. E. Glatt, S. Rief, A. Wiegmann, M. Knefel, E. Wegenke
Structure and pressure drop of real and virtual metal wire meshes
Keywords: metal wire mesh, structure simulation, model calibration, CFD simulation, pressure loss
(7 pages, 2009)

158. S. Kruse, M. Müller
Pricing American call options under the assumption of stochastic dividends – An application of the Korn-Rogers model
Keywords: option pricing, American options, dividends, dividend discount model, Black-Scholes model
(22 pages, 2009)

159. H. Lang, J. Linn, M. Arnold
Multibody dynamics simulation of geometrically exact Cosserat rods
Keywords: flexible multibody dynamics, large deformations, finite rotations, constrained mechanical systems, structural dynamics
(20 pages, 2009)

160. P. Jung, S. Leyendecker, J. Linn, M. Ortiz
Discrete Lagrangian mechanics and geometrically exact Cosserat rods
Keywords: special Cosserat rods, Lagrangian mechanics, Noether's theorem, discrete mechanics, frame-indifference, holonomic constraints
(14 pages, 2009)

161. M. Burger, K. Dreßler, A. Marquardt, M. Speckert
Calculating invariant loads for system simulation in vehicle engineering
Keywords: iterative learning control, optimal control theory, differential algebraic equations (DAEs)
(18 pages, 2009)

162. M. Speckert, N. Ruf, K. Dreßler
Undesired drift of multibody models excited by measured accelerations or forces
Keywords: multibody simulation, full vehicle model, force-based simulation, drift due to noise
(19 pages, 2009)

163. A. Streit, K. Dreßler, M. Speckert, J. Lichter, T. Zenner, P. Bach
Anwendung statistischer Methoden zur Erstellung von Nutzungsprofilen für die Auslegung von Mobilbaggern
Keywords: Nutzungsvielfalt, Kundenbeanspruchung, Bemessungsgrundlagen
(13 pages, 2009)

164. I. Correia, S. Nickel, F. Saldanha-da-Gama
The capacitated single-allocation hub location problem revisited: A note on a classical formulation
Keywords: Capacitated Hub Location, MIP formulations
(10 pages, 2009)

165. F. Yaneva, T. Grebe, A. Scherrer
An alternative view on global radiotherapy optimization problems
Keywords: radiotherapy planning, path-connected sublevelsets, modified gradient projection method, improving and feasible directions
(14 pages, 2009)

166. J. I. Serna, M. Monz, K.-H. Küfer, C. Thieke
Trade-off bounds and their effect in multi-criteria IMRT planning
Keywords: trade-off bounds, multi-criteria optimization, IMRT, Pareto surface
(15 pages, 2009)

167. W. Arne, N. Marheineke, A. Meister, R. Wegener
Numerical analysis of Cosserat rod and string models for viscous jets in rotational spinning processes
Keywords: Rotational spinning process, curved viscous fibers, asymptotic Cosserat models, boundary value problem, existence of numerical solutions
(18 pages, 2009)

168. T. Melo, S. Nickel, F. Saldanha-da-Gama
An LP-rounding heuristic to solve a multi-period facility relocation problem
Keywords: supply chain design, heuristic, linear programming, rounding
(37 pages, 2009)

169. I. Correia, S. Nickel, F. Saldanha-da-Gama
Single-allocation hub location problems with capacity choices
Keywords: hub location, capacity decisions, MILP formulations
(27 pages, 2009)

170. S. Acar, K. Natcheva-Acar
A guide on the implementation of the Heath-Jarrow-Morton Two-Factor Gaussian Short Rate Model (HJM-G2++)
Keywords: short rate model, two factor Gaussian, G2++, option pricing, calibration
(30 pages, 2009)

171. A. Szimayer, G. Dimitroff, S. Lorenz
A parsimonious multi-asset Heston model: calibration and derivative pricing
Keywords: Heston model, multi-asset, option pricing, calibration, correlation
(28 pages, 2009)

172. N. Marheineke, R. Wegener
Modeling and validation of a stochastic drag for fibers in turbulent flows
Keywords: fiber-fluid interactions, long slender fibers, turbulence modelling, aerodynamic drag, dimensional analysis, data interpolation, stochastic partial differential algebraic equation, numerical simulations, experimental validations
(19 pages, 2009)

173. S. Nickel, M. Schröder, J. Steeg
Planning for home health care services
Keywords: home health care, route planning, metaheuristics, constraint programming
(23 pages, 2009)

174. G. Dimitroff, A. Szimayer, A. Wagner
Quanto option pricing in the parsimonious Heston model
Keywords: Heston model, multi asset, quanto options, option pricing
(14 pages, 2009) 174. G. Dimitroff, A. Szimayer, A. Wagner

175. S. Herkt, K. Dreßler, R. Pinnau
Model reduction of nonlinear problems in structural mechanics
Keywords: flexible bodies, FEM, nonlinear model reduction, POD
(13 pages, 2009)

176. M. K. Ahmad, S. Didas, J. Iqbal

Using the Sharp Operator for edge detection and nonlinear diffusion

Keywords: maximal function, sharp function, image processing, edge detection, nonlinear diffusion

(17 pages, 2009)

177. M. Speckert, N. Ruf, K. Dreßler, R. Müller, C. Weber, S. Weihe

Ein neuer Ansatz zur Ermittlung von Erprobungslasten für sicherheitsrelevante Bauteile

Keywords: sicherheitsrelevante Bauteile, Kundenbeanspruchung, Festigkeitsverteilung, Ausfallwahrscheinlichkeit, Konfidenz, statistische Unsicherheit, Sicherheitsfaktoren

(16 pages, 2009)

178. J. Jegorovs

Wave based method: new applicability areas

Keywords: Elliptic boundary value problems, inhomogeneous Helmholtz type differential equations in bounded domains, numerical methods, wave based method, uniform B-splines

(10 pages, 2009)

179. H. Lang, M. Arnold

Numerical aspects in the dynamic simulation of geometrically exact rods

Keywords: Kirchhoff and Cosserat rods, geometrically exact rods, deformable bodies, multibody dynamics, artial differential algebraic equations, method of lines, time integration

(21 pages, 2009)

180. H. Lang

Comparison of quaternionic and rotationfree null space formalisms for multibody dynamics

Keywords: Parametrisation of rotations, differentialalgebraic equations, multibody dynamics, constrained mechanical systems, Lagrangian mechanics

(40 pages, 2010)

181. S. Nickel, F. Saldanha-da-Gama, H.-P. Ziegler

Stochastic programming approaches for risk aware supply chain network design problems

Keywords: Supply Chain Management, multi-stage stochastic programming, financial decisions, risk

(37 pages, 2010)

182. P. Ruckdeschel, N. Horbenko

Robustness properties of estimators in generalized Pareto Models

Keywords: global robustness, local robustness, finite sample breakdown point, generalized Pareto distribution

(58 pages, 2010)

183. P. Jung, S. Leyendecker, J. Linn, M. Ortiz

A discrete mechanics approach to Cosserat rod theory – Part 1: static equilibria

Keywords: Special Cosserat rods; Lagrangian mechanics; Noether's theorem; discrete mechanics; frameindifference; holonomic constraints; variational formulation

(35 pages, 2010)

184. R. Eymard, G. Printsypar

A proof of convergence of a finite volume scheme for modified steady Richards' equation describing transport processes in the pressing section of a paper machine

Keywords: flow in porous media, steady Richards' equation, finite volume methods, convergence of approximate solution

(14 pages, 2010)

185. P. Ruckdeschel

Optimally Robust Kalman Filtering

Keywords: robustness, Kalman Filter, innovation outlier, additive outlier

(42 pages, 2010)

186. S. Repke, N. Marheineke, R. Pinnau

On adjoint-based optimization of a free surface Stokes flow

Keywords: film casting process, thin films, free surface Stokes flow, optimal control, Lagrange formalism

(13 pages, 2010)

187. O. Iliev, R. Lazarov, J. Willems

Variational multiscale Finite Element Method for flows in highly porous media

Keywords: numerical upscaling, flow in heterogeneous porous media, Brinkman equations, Darcy's law, subgrid approximation, discontinuous Galerkin mixed FEM

(21 pages, 2010)

188. S. Desmettre, A. Szimayer

Work effort, consumption, and portfolio selection: When the occupational choice matters

Keywords: portfolio choice, work effort, consumption, occupational choice

(34 pages, 2010)

189. O. Iliev, Z. Lakdawala, V. Starikovicius

On a numerical subgrid upscaling algorithm for Stokes-Brinkman equations

Keywords: Stokes-Brinkman equations, subgrid approach, multiscale problems, numerical upscaling

(27 pages, 2010)

190. A. Latz, J. Zausch, O. Iliev

Modeling of species and charge transport in Li-Ion Batteries based on non-equilibrium thermodynamics

Keywords: lithium-ion battery, battery modeling, electrochemical simulation, concentrated electrolyte, ion transport

(8 pages, 2010)

191. P. Popov, Y. Vutov, S. Margenov, O. Iliev

Finite volume discretization of equations describing nonlinear diffusion in Li-Ion batteries

Keywords: nonlinear diffusion, finite volume discretization, Newton method, Li-Ion batteries

(9 pages, 2010)

192. W. Arne, N. Marheineke, R. Wegener

Asymptotic transition from Cosserat rod to string models for curved viscous inertial jets

Keywords: rotational spinning processes; inertial and viscous-inertial fiber regimes; asymptotic limits; slenderbody theory; boundary value problems

(23 pages, 2010)

193. L. Engelhardt, M. Burger, G. Bitsch

Real-time simulation of multibody-systems for on-board applications

Keywords: multibody system simulation, real-time simulation, on-board simulation, Rosenbrock methods

(10 pages, 2010)

194. M. Burger, M. Speckert, K. Dreßler

Optimal control methods for the calculation of invariant excitation signals for multibody systems

Keywords: optimal control, optimization, mbs simulation, invariant excitation

(9 pages, 2010)

195. A. Latz, J. Zausch

Thermodynamic consistent transport theory of Li-Ion batteries

Keywords: Li-Ion batteries, nonequilibrium thermodynamics, thermal transport, modeling

(18 pages, 2010)

196. S. Desmettre

Optimal investment for executive stockholders with exponential utility

Keywords: portfolio choice, executive stockholder, work effort, exponential utility

(24 pages, 2010)

197. W. Arne, N. Marheineke, J. Schnebele, R. Wegener

Fluid-fiber-interactions in rotational spinning process of glass wool production

Keywords: Rotational spinning process, viscous thermal jets, fluid-fiber-interactions, two-way coupling, slenderbody theory, Cosserat rods, drag models, boundary value problem, continuation method

(20 pages, 2010)

198. A. Klar, J. Maringer, R. Wegener

A 3d model for fiber lay-down in nonwoven production processes

Keywords: fiber dynamics, Fokker-Planck equations, diffusion limits

(15 pages, 2010)

199. Ch. Erlwein, M. Müller

A regime-switching regression model for hedge funds

Keywords: switching regression model, Hedge funds, optimal parameter estimation, filtering

(26 pages, 2011)

200. M. Dalheimer

Power to the people – Das Stromnetz der Zukunft

Keywords: Smart Grid, Stromnetz, Erneuerbare Energien, Demand-Side Management

(27 pages, 2011)

201. D. Stahl, J. Hauth

PF-MPC: Particle Filter-Model Predictive Control

Keywords: Model Predictive Control, Particle Filter, CSTR, Inverted Pendulum, Nonlinear Systems, Sequential Monte Carlo

(40 pages, 2011)

202. G. Dimitroff, J. de Kock

Calibrating and completing the volatility cube in the SABR Model

Keywords: stochastic volatility, SABR, volatility cube, swaption

(12 pages, 2011)

203. J.-P. Kreiss, T. Zangmeister

Quantification of the effectiveness of a safety function in passenger vehicles on the basis of real-world accident data

Keywords: logistic regression, safety function, real-world accident data, statistical modeling

(23 pages, 2011)

204. P. Ruckdeschel, T. Sayer, A. Szimayer

Pricing American options in the Heston model: a close look on incorporating correlation

Keywords: Heston model, American options, moment matching, correlation, tree method

(30 pages, 2011)

205. H. Ackermann, H. Ewe, K.-H. Küfer,
M. Schröder
Modeling profit sharing in combinatorial exchanges by network flows
Keywords: Algorithmic game theory, profit sharing, combinatorial exchange, network flows, budget balance, core
(17 pages, 2011)

206. O. Iliev, G. Printsypar, S. Rief
A one-dimensional model of the pressing section of a paper machine including dynamic capillary effects
Keywords: steady modified Richards' equation, finite volume method, dynamic capillary pressure, pressing section of a paper machine
(29 pages, 2011)

207. I. Vecchio, K. Schladitz, M. Godehardt,
M. J. Heneka
Geometric characterization of particles in 3d with an application to technical cleanliness
Keywords: intrinsic volumes, isoperimetric shape factors, bounding box, elongation, geodesic distance, technical cleanliness
(21 pages, 2011)

208. M. Burger, K. Dreßler, M. Speckert
Invariant input loads for full vehicle multibody system simulation
Keywords: multibody systems, full-vehicle simulation, optimal control
(8 pages, 2011)

209. H. Lang, J. Linn, M. Arnold
Multibody dynamics simulation of geometrically exact Cosserat rods
Keywords: flexible multibody dynamics, large deformations, finite rotations, constrained mechanical systems, structural dynamics
(28 pages, 2011)

210. G. Printsypar, R. Ciegis
On convergence of a discrete problem describing transport processes in the pressing section of a paper machine including dynamic capillary effects: one-dimensional case
Keywords: saturated and unsaturated fluid flow in porous media, Richards' approach, dynamic capillary pressure, finite volume methods, convergence of approximate solution
(24 pages, 2011)

211. O. Iliev, G. Printsypar, S. Rief
A two-cimensional model of the pressing section of a paper machine including dynamic capillary effects
Keywords: two-phase flow in porous media, steady modified Richards' equation, finite volume method, dynamic capillary pressure, pressing section of a paper machine, multipoint flux approximation
(44 pages, 2012)

212. M. Buck, O. Iliev, H. Andrä
Multiscale finite element coarse spaces for the analysis of linear elastic composites
Keywords: linear elasticity, domain decomposition, multiscale finite elements, robust coarse spaces, rigid body modes, discontinuous coefficients
(31 pages, 2012)

213. A. Wagner
Residual demand modeling and application to electricity pricing
Keywords: residual demand modeling, renewable infeed, wind infeed, solar infeed, electricity demand, German power market, merit-order effect
(28 pages, 2012)

214. O. Iliev, A. Latz, J. Zausch, S. Zhang
An overview on the usage of some model reduction approaches for simulations of Li-ion transport in batteries
Keywords: Li-ion batteries, porous electrode model, model reduction
(21 pages, 2012)

215. C. Zémerli, A. Latz, H. Andrä
Constitutive models for static granular systems and focus to the Jiang-Liu hyperelastic law
Keywords: granular elasticity, constitutive modelling, non-linear finite element method
(33 pages, 2012)

216. T. Gornak, J. L. Guermond, O. Iliev,
P. D. Minev
A direction splitting approach for incompressible Brinkmann flow
Keywords: unsteady Navier-Stokes-Brinkman equations, direction splitting algorithms, nuclear reactors safety simulations
(16 pages, 2012)

217. Y. Efendiev, O. Iliev, C. Kronsbein
Multilevel Monte Carlo methods using ensemble level mixed MsFEM for two-phase flow and transport simulations
Keywords: two phase flow in porous media, uncertainty quantification, multilevel Monte Carlo
(28 pages, 2012)

218. J. Linn, H. Lang, A. Tuganov
Geometrically exact Cosserat rods with Kelvin-Voigt type viscous damping
Keywords: geometrically exact rods, viscous damping, Kelvin-Voigt model, material damping parameters
(10 pages, 2012)

Status quo: October 2012